Electronic Supplementary Material (ESI) for ChemComm.

Supporting Information for

In-situ utilization of photogenerated hydrogen for hydrogenation reaction over covalent organic framework

Guang-Bo Wang,† Ke-Hui, Xie,† Jing-Lan Kan, Hai-Peng Xu, Fei Zhao, Yan-Jing Wang, Yan Geng* and Yu-Bin Dong*

College of Chemistry, Chemical Engineering and Materials Science, Collaborative Innovation Center of Functionalized Probes for Chemical Imaging in Universities of Shandong, Key Laboratory of Molecular and Nano Probes, Ministry of Education, Shandong Normal University, Jinan 250014, P. R. China.

† These authors contributed equally to this work.

Materials and methods

All the chemicals were purchased from commercial suppliers and used without further purification unless otherwise noted. The building block of 2,2'-(2',5'-difluoro-[1,1':4',1''-terphenyl]-4,4''-diyl)diacetonitrile (FTPDAN) was synthesized as follows.

^{1}H and ^{13}C NMR spectra were recorded on a Bruker Avance 400 NMR spectrometer. Fourier Transform Infrared (FT-IR) spectra in the region of 800-4000 cm^{-1} were obtained with a Perkin-Elmer 1600 FT-IR spectrometer. Powder X-ray diffraction (PXRD) data were collected using a D8 ADVANCE X-ray with Cu K_{α} radiation (λ = 1.05405 Å). Thermogravimetric analysis (TGA) was performed on Mettler Toledo TGA/DSC 3+ with the temperature ranging from 20 to 800 °C under nitrogen and a heating rate of 10 °C/min. Solid state ^{13}C CP-MAS NMR spectrum was measured at 125.7 MHz using a 4 mm MAS NMR probe with a spinning rate of 8 kHz. Scanning electron microscopy (SEM) images of the **Py-FTP-COF** materials were carried out on a SUB010 scanning electron microscope with acceleration voltage of 20 kV and the transmission electron microscopy (TEM) analysis was performed on a JEOL 2100 Electron Microscope with an operating voltage of 200 kV. Solid state UV-Vis spectra were recorded on a Cary 5000 UV-Vis spectrophotometer (Varian, USA). N_2 adsorption measurements were performed using an ASAP 2460 apparatus at 77 K, the samples were degassed under high vacuum at 120 ºC for 8h before analysis.

Cyclic voltammetry (CV) measurements were performed on a CHI 660E in a three-electrode electrochemical cell equipped with a salt bridge and a scan rate of 100 mVs^{-1}. The photocurrent measurements were conducted on a workstation in a standard three-electrode system in dark and light excitation at -0.14 V vs. Ag/AgCl with the photocatalyst-coated FTO as the working electrode, Pt plate as the counter electrode and Ag/AgCl as the reference electrode by directly irradiating the working electrode from the back side using a 300 W Xe lamp and 2M Na_2SO_4 aqueous solution was used as the electrolyte. Electrochemical impedance spectroscopy (EIS) analysis was performed at the open circuit condition at -0.14 V vs. Ag/AgCl in the frequency range of 0.01 to 10000 Hz with an AC amplitude of 10 mV.

Synthesis of 2,2'-(2',5'-difluoro-[1,1':4',1''-terphenyl]-4,4''-diyl)diacetonitrile (FTPDAN)

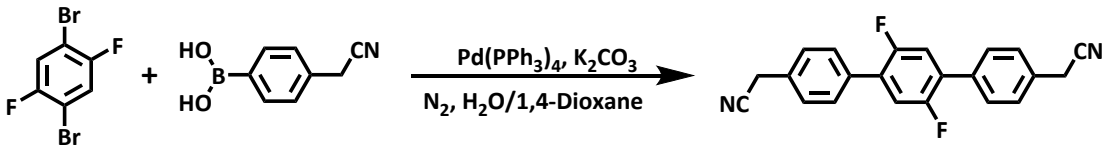

In general, K_2CO_3 (11.04 mmol, 1.7 g), 1,4-dibromo-2,5-difluorobenzene (3.7 mmol, 1.0 g) and 4-Cyanomethylbenzeneboronc acid (10.56 mmol, 1.5 g) were introduced into a 250 mL three-necked flask and degassed for three times. Then, degassed H_2O/anhydrous 1,4-dioxane (1:4, v/v, 125 mL) and $Pd(PPh_3)_4$ (0.42 mmol, 0.46 g) were slowly added into the flask under N_2 atmosphere. After reflux for 24h under N_2, the mixture was poured into distilled water, extracted with chloroform, dried over anhydrous $MgSO_4$ and evaporated under reduced pressure, giving the crude compound, which was further purified by flash chromatography with dichloromethane as eluent to afford the targeted product as a white powder (0.85 g, 72%). ^{1}H NMR (400 MHz, DMSO-d_6) δ 7.67 (d, J = 8.0 Hz, 4H), 7.58 (t, J = 8.9 Hz, 2H), 7.49 (d, J = 8.2 Hz, 4H), 4.12 (s, 4H). ^{13}C NMR (101 MHz, DMSO-d_6) δ 156.89, 154.46, 133.43, 132.12, 129.83, 128.98, 119.59, 118.27, 117.96.

HRMS (ESI) calculated for $C_{22}H_{14}F_2N_2$ [M + Na]: 367.1023, Found: 367.0999.

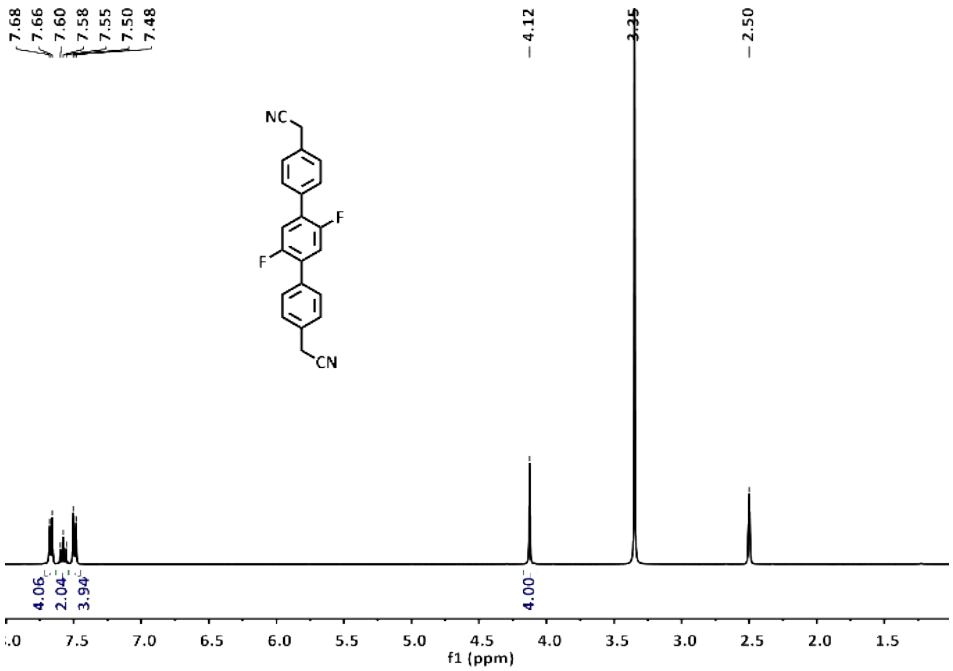

Figure S1. ^{1}H NMR spectrum of the FTPDAN (DMSO-d_6).

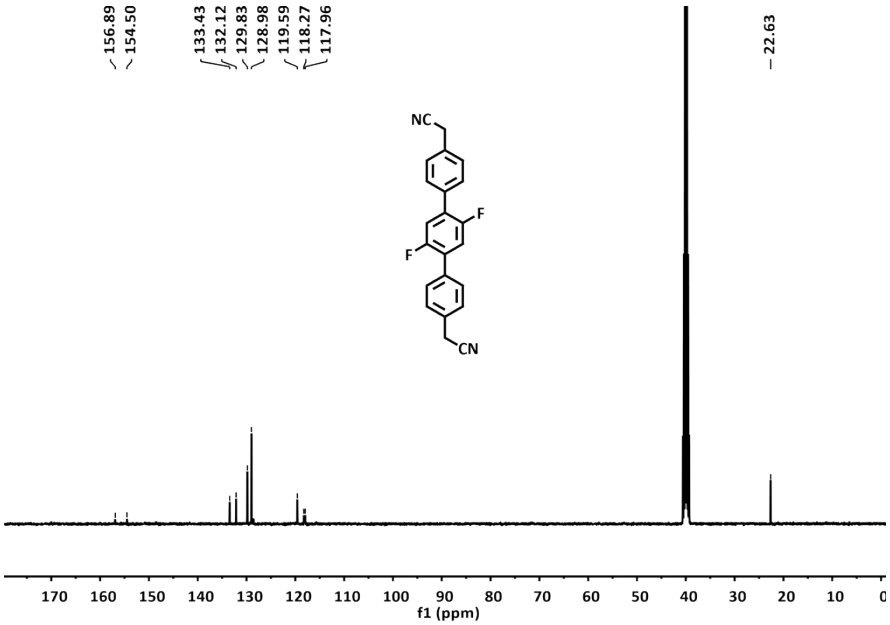

Figure S2. ^{13}C NMR spectrum of the FTPDAN (DMSO-d_6).

Synthesis of the Py-FTP-COF

Py-CHO (0.03 mmol, 18.6 mg) and FTPDAN (0.06 mmol, 20.66 mg) was added into a 10 mL Pyrex tube, followed by the addition of 1,2-dichlorobenzene (*o*-DCB, 2 mL), H_2O (0.1 mL) and TBAH catalyst (1 M in MeOH, 200 µL). Afterwards, the mixture was homogenized by sonication for 5 minutes and the Pyrex tube was flash frozen at 77 K (liquid N_2 bath) and degassed by three-freeze-pump-thaw cycles for three times, sealed under vacuum and then heated at 120 ºC for 5 days. After cooling down to room temperature, the precipitate was collected by centrifugation and washed with N, N-dimethylformamide, THF, acetone and dried under vacuum at 100 ºC to afford the yellow powders. (35 mg, 90%).

Photocatalytic H_2 evolution experiments

For a typical H_2 evolution experiment, a Pyrex tube was charged with the activated COF powder (5 mg), 0.1 M ascorbic acid water solution (10 mL) and hexachloroplatinic acid solution as the platinum precursor. After deoxygenation with argon for 30 min, CH_4 gas is injected into the tube as an internal standard to quantify the amount of photogenerated H_2 gas. The system was connected to the device and irradiated with a 300 W Xenon lamp equipped with an under constant agitation and fan cooling for real time quantitative hydrogen detection. The generated H_2 was quantitatively measured by drainage gas-collecting and analyzed by gas chromatography (Fuli, 9790 II (PLF-01)) equipped with a

thermal conductive detector (TCD) and a 5 Å molecular sieve column with argon as the carrier gas. After the photocatalysis experiments, the COF material was recovered by washing with water and acetone then dried under vacuum at 120 ºC for multiple runs.

Tandem photocatalytic hydrogenation of nitroarenes.

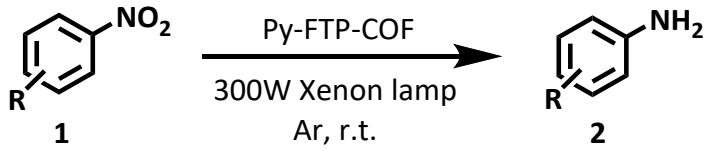

For a typical tandem reaction, a Pyrex tube was charged with the activated **Py-FTP-COF** (5 mg, 15 mol%), nitrobenzene (10.2 µL, 0.1 mmol), 10 mL 0.1 M ascorbic acid water solution and CH_3OH mixture (1:1, v/v) and 4 µL hexachloroplatinic acid solution. After deoxygenation with argon for 20 min, the solution was then thoroughly degassed and irradiated using a Microsolar300 Xe lamp for 4 h. After completion of the reaction, the **Py-FTP-COF** was collected by centrifugation and washed thoroughly with water and methanol, reactivated under vacuum at 100 ºC for recycling tests. The solution was concentrated in vacuo, and the residue was purified by column chromatography on silica gel to get the products.

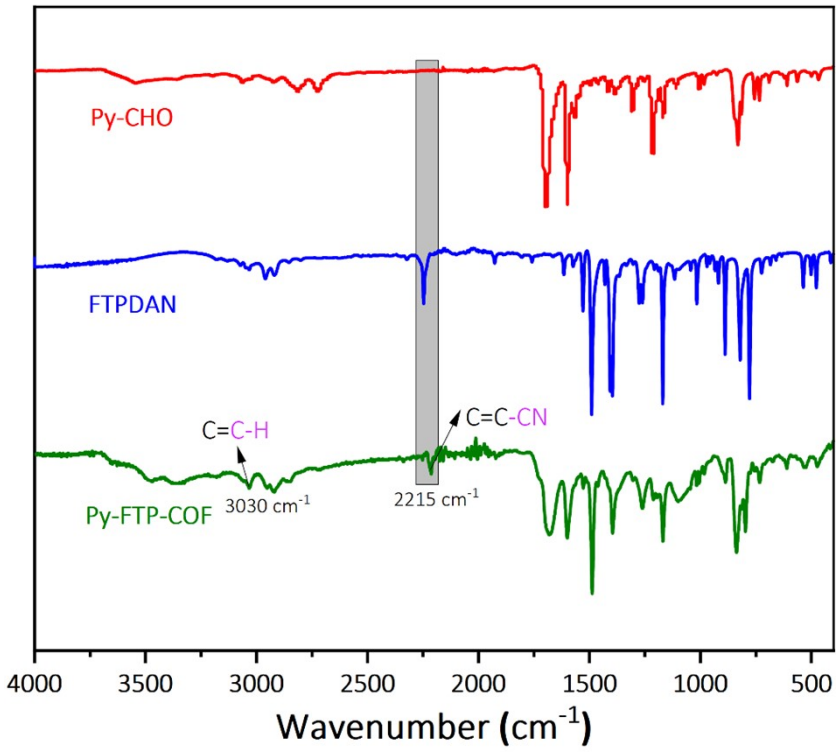

Figure S3. FT-IR spectra of Py-CHO (red), FTPDAN (blue) and the **Py-FTP-COF** (green).

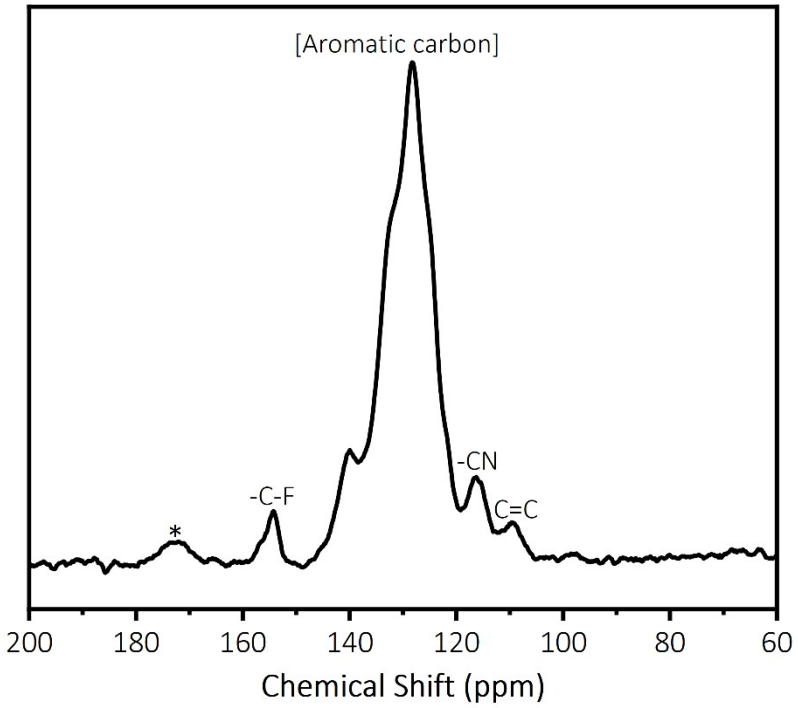

Figure S4. The solid state ^{13}C cross polarization magic angle spinning (^{13}C CP/MAS) NMR spectrum of **Py-FTP-COF** (Asterisk is the spinning sideband).

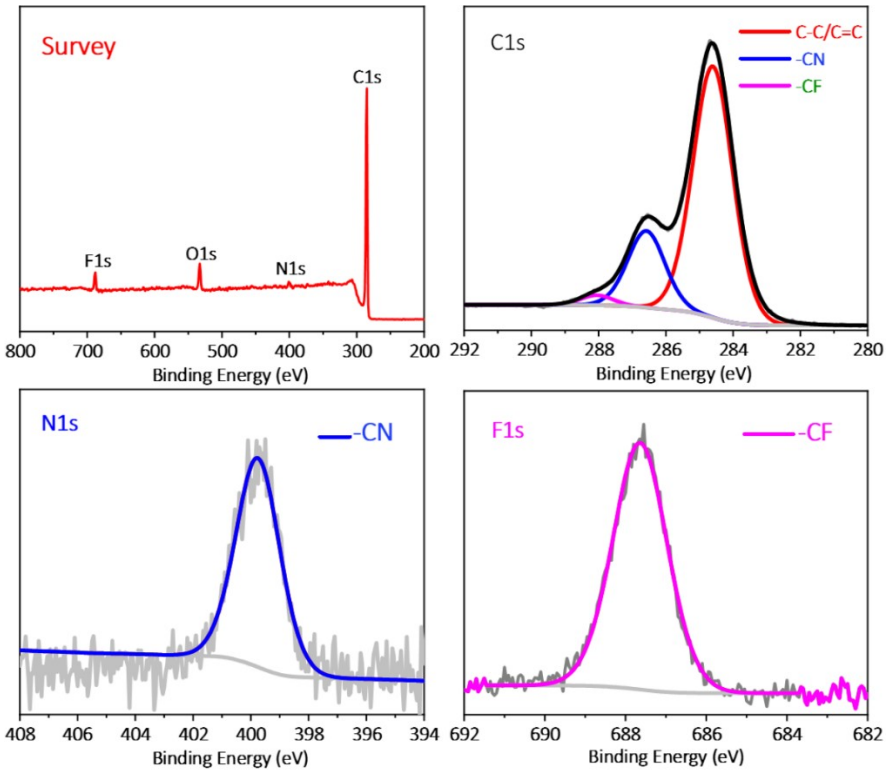

Figure S5. XPS spectra of the **Py-FTP-COF**. According to the C1s spectrum, the signals at 284.5 ± 0.1 eV, 286.1 ± 0.1 eV and 288.1 ± 0.1 eV can be ascribed to the olefin carbon, cyano

carbon and C-F carbon, respectively, while the characteristic peaks at 399.7 ± 0.1 eV in the N1s spectrum originating from the cyano groups and at 687.6 ± 0.1 eV arising from the C-F bonds in the F1s spectrum can also be clearly observed.

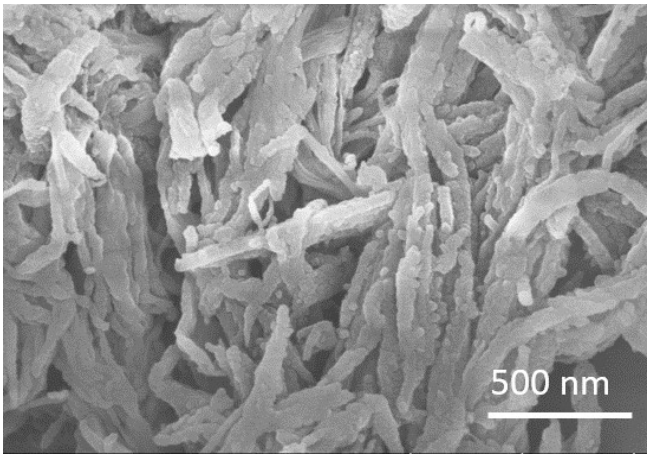

Figure S6. Scanning electron microscopy (SEM) image of the **Py-FTP-COF.**

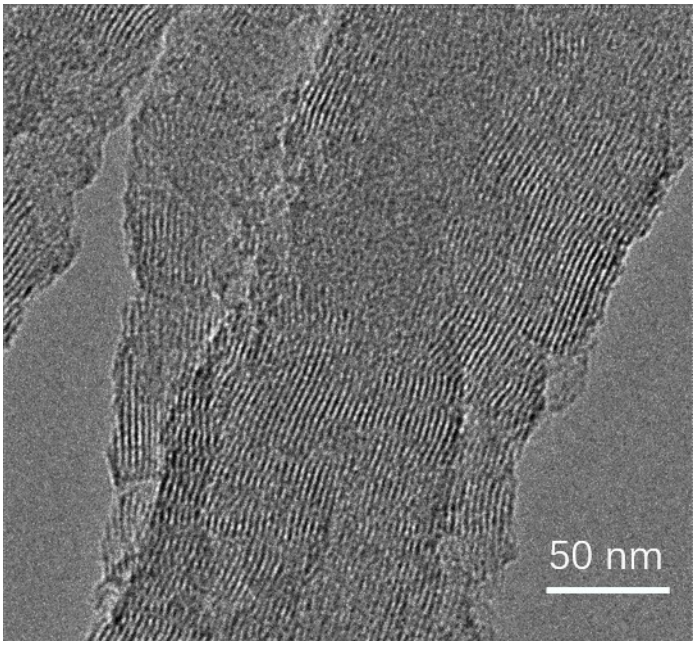

Figure S7. Transmission electron microscopy (TEM) image of the **Py-FTP-COF**.

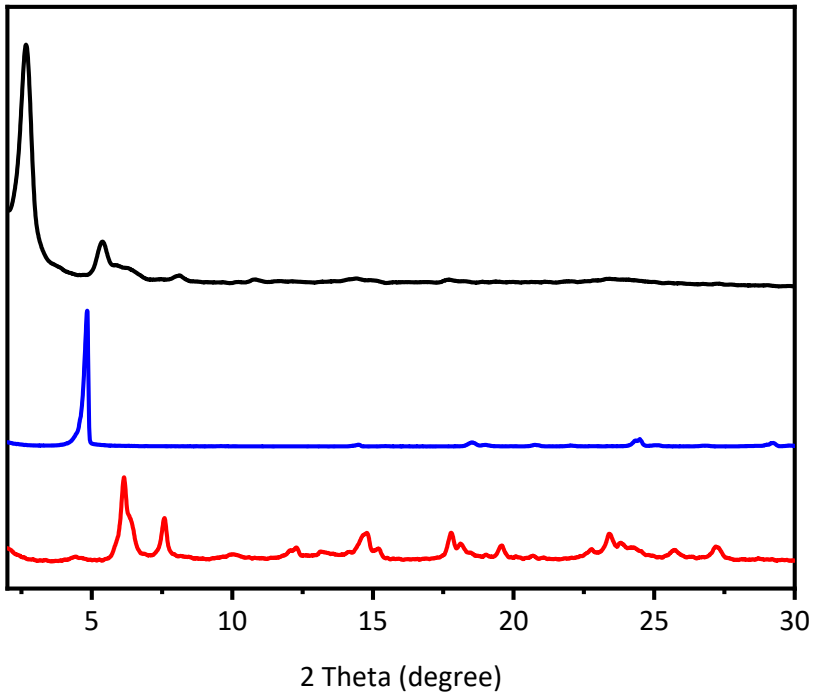

Figure S8. Comparison of the PXRD patterns of Py-CHO (red), FTPDAN (blue) and **Py-FTP-COF** (black).

Table S1. Fractional atomic coordinates for the unit cell of **Py-FTP-COF** with AA stacking.

Space group: *PM*			
a = 49.7458Å, b = 43.8086Å, c = 3.843Å			
α = γ = 90º, β = 91.2723º			
C1	2.52488	-1.53262	-0.05785
C2	2.54878	-1.51587	-0.13821
C3	2.47525	-1.5649	0.01151
C4	2.54966	-1.58446	-0.02166
C5	2.55094	-1.61358	-0.18022
C6	2.57383	-1.63201	-0.18595
C7	2.59635	-1.62179	-0.03689
C8	2.59526	-1.59286	0.12006
C9	2.57198	-1.57496	0.13811
C10	2.62188	-1.63961	-0.06157
C11	2.19762	-1.78216	0.10174
C12	2.22371	-1.76543	0.11202
C13	2.27373	-1.73438	0.12183

C14	2.29991	-1.71761	0.11918
C15	2.32393	-1.72918	-0.06472
C16	2.34834	-1.7137	-0.06385
C17	2.34944	-1.68561	0.11035
C18	2.32545	-1.67358	0.28806
C19	2.3011	-1.68945	0.29464
C20	2.3758	-1.66985	0.11466
C21	2.02284	-1.96744	0.05872
C22	2.02347	-1.93502	0.03804
C23	2.04408	-1.98413	0.17005
C24	2.04828	-1.91638	0.06651
C25	2.07337	-1.92484	-0.11608
C26	2.09619	-1.90669	-0.10387
C27	2.09449	-1.87894	0.07977
C28	2.06953	-1.87043	0.26528
C29	2.04671	-1.88875	0.25557
C30	2.11957	-1.86074	0.09001
C31	2.1215	-1.8299	0.07897
C32	2.14793	-1.8138	0.08697
C33	2.16909	-1.82703	0.2428
C34	2.19346	-1.81148	0.25013
C35	2.17657	-1.76911	-0.05666
C36	2.15214	-1.78445	-0.06042
C37	2.24942	-1.71814	0.1326
C38	2.22479	-1.73328	0.13612
C39	2.24803	-1.78166	0.10163
C40	2.27251	-1.76658	0.11467
F41	2.20205	-1.71618	0.17488
F42	2.29477	-1.78381	0.13133
C43	1.00003	1.08043	0.97478
C44	1	1.01632	0.9755
C45	2.50021	-1.51634	-0.03601
C46	2.4997	-1.58005	0.03115
C47	2.45245	-1.51587	-0.07459
C48	2.47561	-1.53256	-0.02717
C49	2.52471	-1.56504	-0.01736
C50	2.45014	-1.58407	0.03452
C51	2.42611	-1.57545	0.24266
C52	2.4029	-1.59342	0.25551
C53	2.4034	-1.6214	0.07751
C54	2.42751	-1.63056	-0.12405
C55	2.45051	-1.61217	-0.14486
C56	2.37799	-1.63919	0.08458
C57	2.97656	-1.93501	-0.08782
C58	2.97715	-1.96744	-0.1077
C59	2.95588	-1.98413	-0.21817
C60	2.95177	-1.91635	-0.1162
C61	2.95335	-1.88876	-0.3061

C62	2.93059	-1.87035	-0.31478
C63	2.90566	-1.87865	-0.12655
C64	2.90394	-1.90641	0.05731
C65	2.9267	-1.92469	0.0678
C66	2.88063	-1.86025	-0.1331
C67	2.87892	-1.82937	-0.12632
C68	2.85252	-1.81298	-0.12916
C69	2.84926	-1.78286	0.00019
C70	2.82496	-1.76718	-0.00001
C71	2.80293	-1.78105	-0.12683
C72	2.80599	-1.81097	-0.25833
C73	2.83045	-1.8266	-0.26297
C74	2.77674	-1.76461	-0.11708
C75	2.77559	-1.73374	-0.21774
C76	2.75083	-1.71867	-0.20325
C77	2.72658	-1.73382	-0.08688
C78	2.72775	-1.76469	0.01427
C79	2.75251	-1.77979	-0.00173
C80	2.7004	-1.71723	-0.07083
C81	2.69777	-1.68714	0.05747
C82	2.67319	-1.6716	0.07498
C83	2.65056	-1.68569	-0.03734
C84	2.65332	-1.71572	-0.1674
C85	2.67785	-1.73122	-0.18454
C86	2.62385	-1.67002	-0.00871
F87	2.79832	-1.71819	-0.33815
F88	2.70507	-1.78013	0.13942
C89	0.90249	1.1887	0.91329
N90	0.92129	1.2032	0.94586
C91	0.60011	1.31168	1.09261
N92	0.58117	1.29695	1.17394
C93	0.39877	1.31159	1.16747
N94	0.4171	1.29669	1.21046
C95	0.09821	1.18835	1.0307
N96	0.07964	1.20299	0.99127
H97	2.56795	-1.5268	-0.20798
H98	2.53455	-1.62183	-0.31193
H99	2.61225	-1.58442	0.23882
H100	2.5715	-1.55374	0.28023
H101	2.64018	-1.62643	-0.11993
H102	2.32394	-1.74984	-0.21856
H103	2.36636	-1.72341	-0.20758
H104	2.32563	-1.65243	0.43339
H105	2.28335	-1.67992	0.44608
H106	2.06084	-1.97289	0.2649
H107	2.07533	-1.94531	-0.27406
H108	2.11517	-1.914	-0.24669
H109	2.06768	-1.85017	0.42737

H110	2.02788	-1.88147	0.40156
H111	2.13782	-1.87402	0.0824
H112	2.16667	-1.84898	0.3718
H113	2.20867	-1.82217	0.38423
H114	2.1791	-1.74736	-0.18957
H115	2.13679	-1.77348	-0.18978
H116	2.2493	-1.69345	0.13789
H117	2.24829	-1.8063	0.08293
H118	1.00004	1.10513	0.97437
H119	2.49919	-1.60434	0.08387
H120	2.43395	-1.52693	-0.11568
H121	2.4252	-1.55483	0.39758
H122	2.38459	-1.58577	0.41224
H123	2.42833	-1.65125	-0.27877
H124	2.46847	-1.61959	-0.31067
H125	2.35997	-1.62594	0.06755
H126	2.9391	-1.97288	-0.31243
H127	2.97217	-1.88159	-0.45344
H128	2.93245	-1.85017	-0.47816
H129	2.88498	-1.9136	0.20199
H130	2.92472	-1.94514	0.2262
H131	2.86229	-1.87342	-0.11831
H132	2.86538	-1.77133	0.10865
H133	2.82327	-1.74436	0.1077
H134	2.78958	-1.82208	-0.36532
H135	2.83202	-1.84909	-0.37942
H136	2.7506	-1.69512	-0.28832
H137	2.75276	-1.80333	0.08379
H138	2.71459	-1.67586	0.15298
H139	2.67175	-1.64889	0.18656
H140	2.63647	-1.7272	-0.26006
H141	2.67923	-1.75407	-0.29197
H142	0.57427	1.34639	0.67783

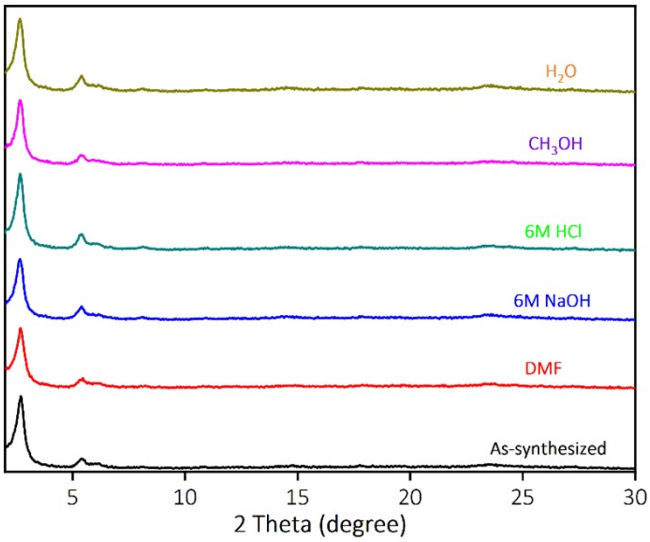

Figure S9. PXRD patterns of the **Py-FTP-COF**: as synthesized, immersed in DMF, 6M NaOH, 6M HCl, CH_3OH and H_2O, respectively.

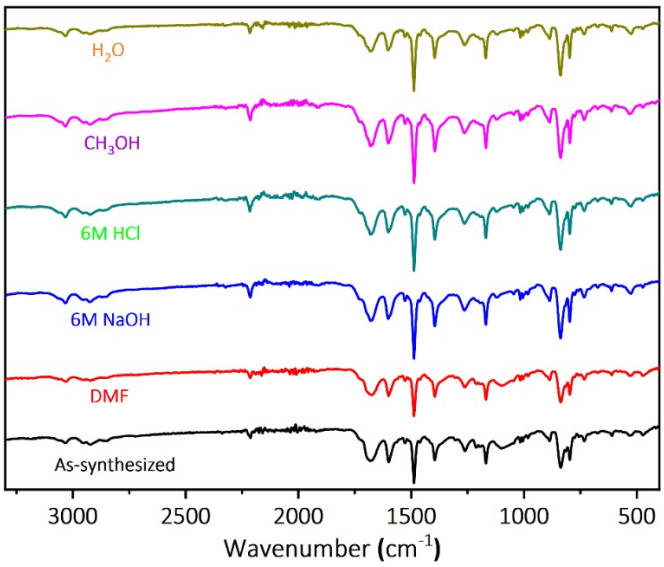

Figure S10. FT-IR spectra of the **Py-FTP-COF**: as synthesized, immersed in DMF, 6M NaOH, 6M HCl, CH_3OH and H_2O, respectively.

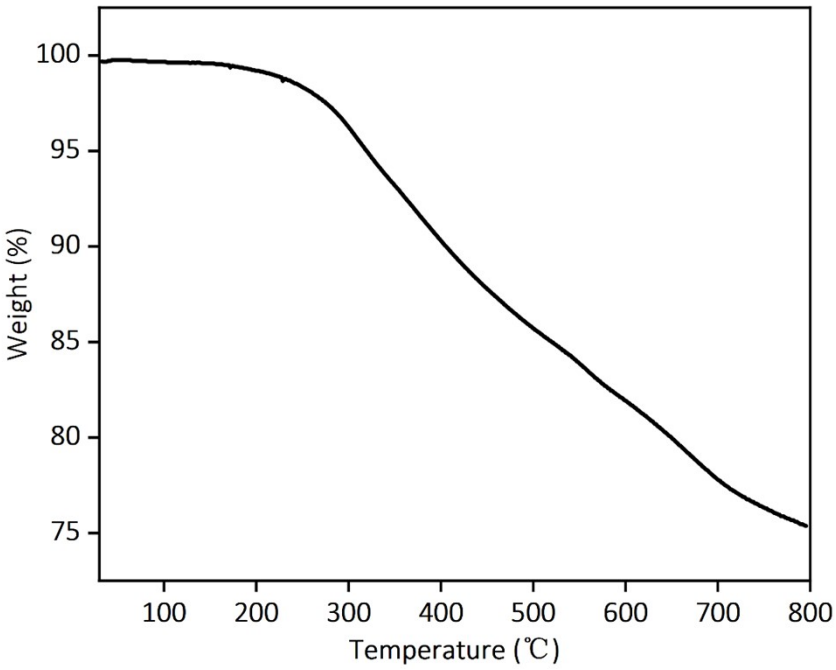

Figure S11. Thermogravimetric analysis (TGA) curve of **Py-FTP-COF** measured under nitrogen flow with a heating rate 10 ℃/min up to 800 ℃.

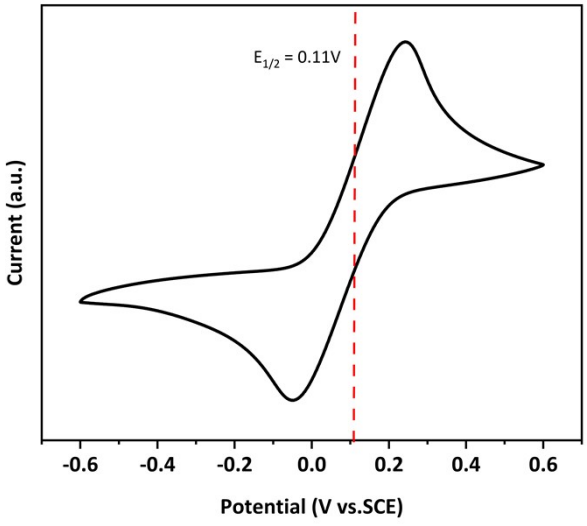

Figure S12. Cyclic voltammetry measurements of ferrocene/ferrocenium couple to calibrate the pseudo reference electrode ($E_{1/2}$ is obtained to be 0.11 V).

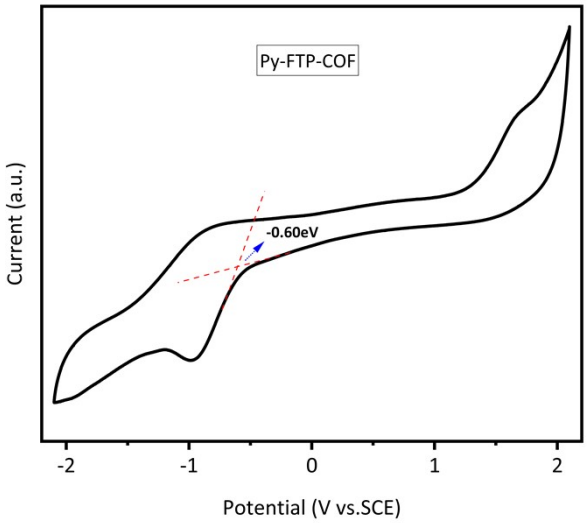

Figure S13. Cyclic voltammetry plot of **Py-FTP-COF** referenced to saturated calomel (SCE) using ferrocene (Fc) as an internal standard at a scan rate of 100 mV S^{-1}. The calculation of the E_{HOMO} and E_{LUMO} is according to the following equations:

$$E_{LUMO} = -\left(E_{onset\ vs.\ SCE} - E_{1/2,Fc} + 4.8\right)eV$$

$$E_{HOMO} = E_{LUMO} - E_{g,opt}$$

Where, $E_{1/2}$, F_c is obtained to be 0.11 vs. SCE., reduction onset potential (E_{onset} vs. SCE) was extracted from the X-intercept of the linear fit in the voltammogram, $E_{g,opt}$ is obtained from the UV-Vis spectrum by using Tauc-plot method.

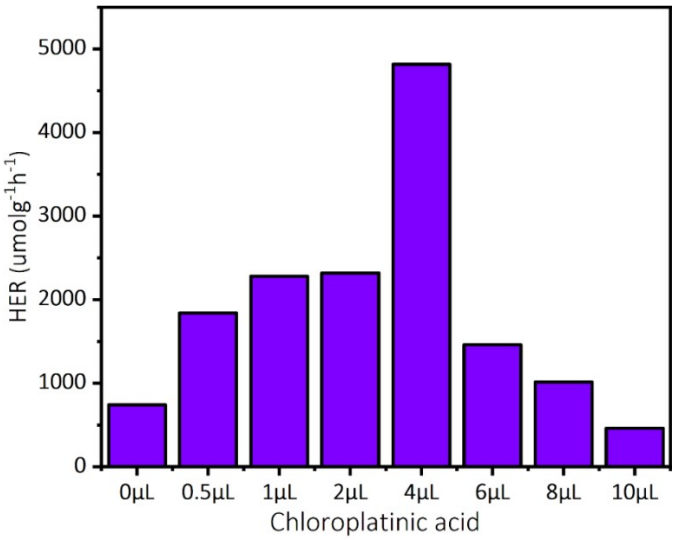

Figure S14. Hydrogen evolution rate versus the amount of the co-catalyst (5 mg **Py-FTP-COF,** 10 mL ascorbic acid water solution (0.1 M), different volumes of the H_2PtCl_4 precursor in 2h under 300 W Xe lamp irradiation). The HER in 2h gradually enhanced with the increase of the amount of the Pt precursor and reached the maximum when 4 μL H_2PtCl_6 was introduced, thus, the detailed photocatalytic reactions were performed under this optimized condition.

Table S2 The summary of the photocatalytic H_2 evolution performance under visible light irradiation over different types of COFs

COFs	Band gap (eV)	Co-catalyst	Sacrificial agent	HER ($\mu molg^{-1}h^{-1}$)	Ref.
g-$C_{40}N_3$-COF	2.36	Pt	Na_2S	4	1
TA-COF	2.82	Pt	TEOA	10	2
g-$C_{40}N_3$-COF	2..36	Pt	TEA	12	1
g-$C_{40}N_3$-COF	2.36	Pt	Na_2SO_3	14	1
N_0-COF	2.6-2.7	Pt	TEOA	23	3
TpPa-2-COF	2.52	Pt	Lactic acid	28	4
g-$C_{40}N_3$-COF	2.36	Pt	EtOH	56	1
TpPa-2	2.07	Pt	Sodium ascorbate	72.09	5
COF-923	1.74	Pt	TEOA	73	6
g-$C_{33}N_3$-COF	2.54	Pt	Ascorbic acid	74	7
BE-COF	2.12	Pt	Ascorbic acid	76	8
TFA-COF	2.40	Pt	TEOA	80	2
PTP-COF	2.1	Pt	TEOA	83.83	9
N_1-COF	2.6-2.7	Pt	TEOA	90	3
N_1-COF	-	Co-1	TEOA	100	10
COF-932	-	Pt	TEOA	110	6
CTP-1	2.96	Pt	TEOA	120	11
sp^2c-CMP	1.96	Pt	TEOA	140	12
TTR-COF	2.71	Au	TEOA	141	13
TTB-COF	2.8	Au	TEOA	145.25	13
N_3-COF	-	Co-1	TEOA	163	10
OB-POP-1	2.21	Pt	TEOA	168	14

CTF-1	2.23	Pt	TEOA	168	15
B-CTF-1	2.14	Pt	TEOA	179	15
TpPa-COF-NO_2	1.92	Pt	Sodium ascorbate	220	16
COF-42	-	Co-1	TEOA	233	10
g-$C_{18}N_3$-COF	2.42	Pt	Ascorbic acid	292	7
TP-BDDA	2.31	Pt	TEOA	324 ± 10	17
CTF-15	2.58	Pt	TEOA	352	18
TBC-COF	-	Pt	TEOA	360	15
N_2-COF	-	Co-2[b]	TEOA	414	10
PyTA-BC-Ph	2.67		Ascorbic acid	417	19
PMDA-COF	1.99	Pt	TEOA	435.6	20
N_2-COF	2.6-2.7	Pt	TEOA	438	3
CTP_{300}	2.36	Pt	TEOA	500	11
TAB-TFP-COF	2.45	Pt	Ascorbic acid	666.4	21
COF-932	-	Pt	Ascorbic acid	730	6
BtCOF150	2.10	Pt	TEOA	750 ± 25	22
N_2-COF	-	Co-1[a]	TEOA	782	10
OB-POP-2	2.28	Pt	TEOA	940	14
TpDTz COF	2.07	NiME	TEOA	941	23
BT-TAPT-COF	2.35	Pt	Ascorbic acid	946	24
PyTA-BC	2.71		Ascorbic acid	1183	19
TpPa-1-COF	2.02	Pt	Sodium ascorbate	1223	25
sp^2c-COF	1.9	Pt	TEOA	1360	12
BDF-TAPT-COF	2.57	Pt	Ascorbic acid	1390	26
TpPa-COF	2.09	Pt	Sodium ascorbate	1560	16
TP-COF	2.28	Pt	Ascorbic acid	1600(±80)	27
N_3-COF	2.6-2.7	Pt	TEOA	1703	3
$Ni(OH)_2$-2.5%/TpPa-2	-	$Ni(OH)_2$	Sodium ascorbate	1895.99	5
TFPT-COF	2.8	Pt	TEOA	1970	28
PyTz-COF	2.20	Pt	Ascorbic acid	2072.4	29
sp^2c-COF_{ERDN}	1.85	Pt	TEOA	2120	12
g-$C_{54}N_6$-COF	2.03	Pt	TEOA	2518.9	30
g-$C_{40}N_3$-COF	2.36	Pt	TEOA	2596	1
Py-FTP-BTCOF	2.34	Pt	Ascorbic acid	2875	31
TpPa-COF-CH_3	2.10	Pt	Sodium ascorbate	3070	16
α-Fe_2O_3/TpPa-2-COF (3:7)	2.07	Pt	Sodium ascorbate	3770	32
CdS-COF (90:10)	-	Pt	Lactic acid	3678	4
S-COF	2.10	Pt	Ascorbic acid	4440 (±140)	26
TpPa-1	2.11	Pt	Ascorbic acid	5479	33
MoS_2-3%/TpPa-1-COF	2.14	MoS2	Ascorbic acid	5585	33
TpPa-COF-$(CH_3)_2$	2.06	Pt	Sodium ascorbate	8330	16
TP-COF	1.97	PVP-Pt	Ascorbic acid	8420	8
Py-ClTP-BT-COF	2.36	Pt	Ascorbic acid	8875	31
CN-COF	2.09	Pt	TEOA	10100	34
TiO_2-TpPa-1-COF (1:3)	2.15	Pt	Sodium ascorbate	11190	35
rGO(5%)-TpPa-1-COF	2.06	Pt	Sodium ascorbate	11980	36
FS-COF	1.85	Pt	Ascorbic acid	10100(±300)	26
Mo_3S_{13}@EB-COF	-	$Ru(bpy)_3Cl_2$	Ascorbic acid	13215	37
FS-COF+WS5F	-	Pt	Ascorbic acid	16300 (±290)	26
USTB-10	1.52	Pt	Ascorbic acid	21800	38
COF-923	-	Pt	Ascorbic acid	23400	6
NH_2-UiO-66/TpPa-1-COF (4:6)	2.10	Pt	Sodium ascorbate	23413	25
WO_3@TpPa-1-COF/rGo (30%)	2.11	Pt	Ascorbic acid	26730	39

Tp-2C/BPy^{2+}-COF (19.10%)		Pt	Ascorbic acid	34600	40
Cu-salphen-HDCOF-NSs+FS	1.62		TEA	36990	41
COF-JLU100	1.4	Pt	TEOA	107380	42

[a] Co-1: [Co(dmgH)$_2$pyCl]; [b]Co-2: [Co(dmgBF$_2$)$_2$(OH$_2$)$_2$]; [c] PE: Photonic efficiency; TEOA: Triethanolamine; TEA: Triethylamine.

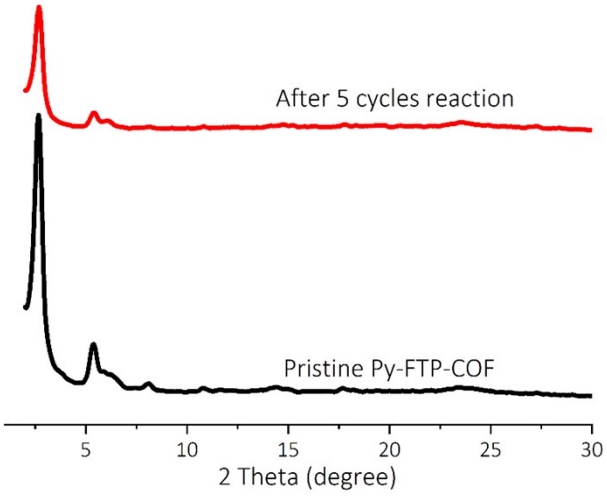

Figure S15. PXRD patterns of the **Py-FTP-COF** before and after 5 cycles reactions.

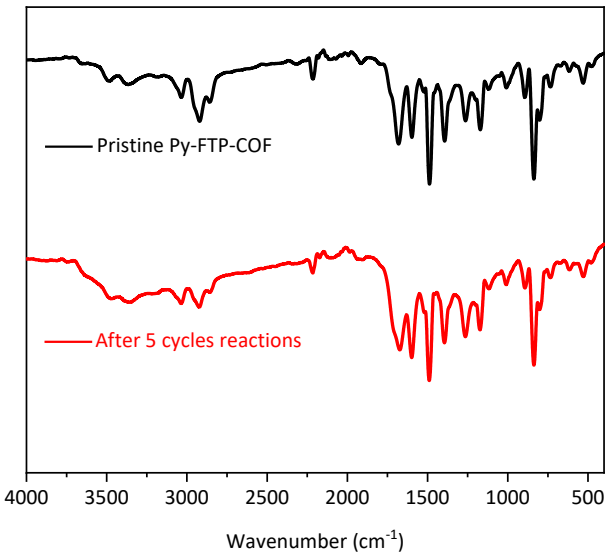

Figure S16. FT-IR spectra of the **Py-FTP-COF** before and after 5 cycles reactions.

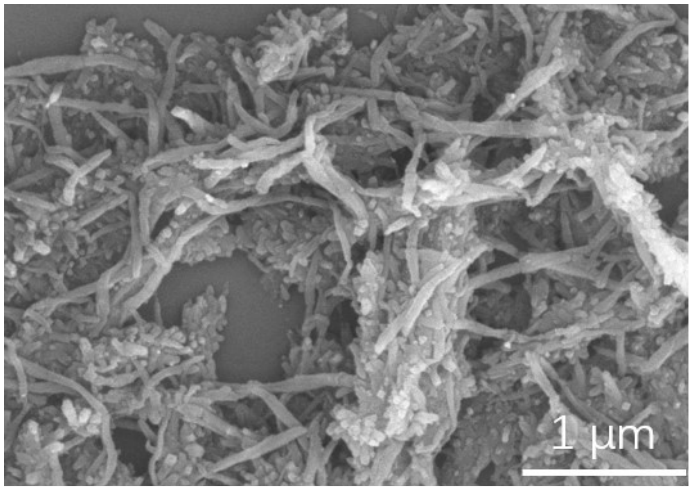

Figure S17. SEM images of the **Py-FTP-COF** after 5 cycles photocatalytic hydrogen evolution.

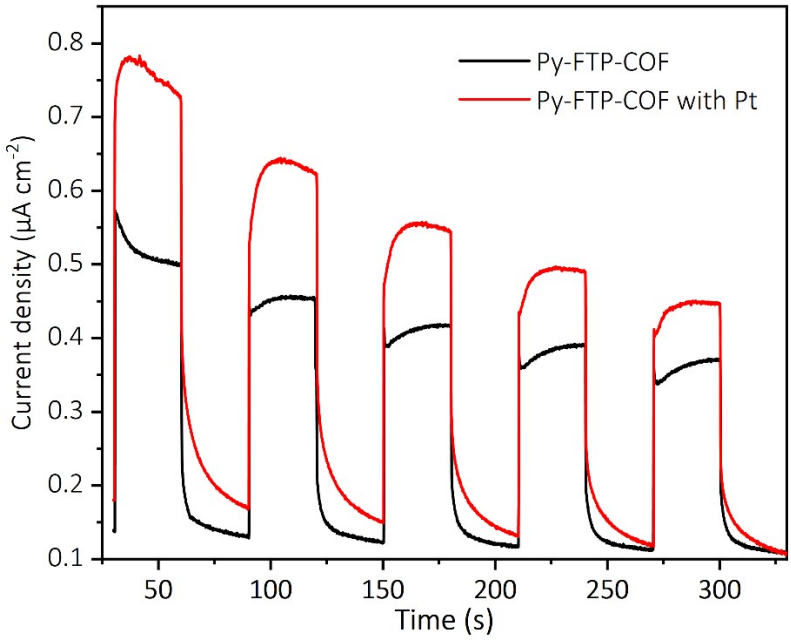

Figure S18. Photocurrent responses (i–t) of the **Py-FTP-COF** photocatalysts in the presence or absence of the Pt co-catalyst.

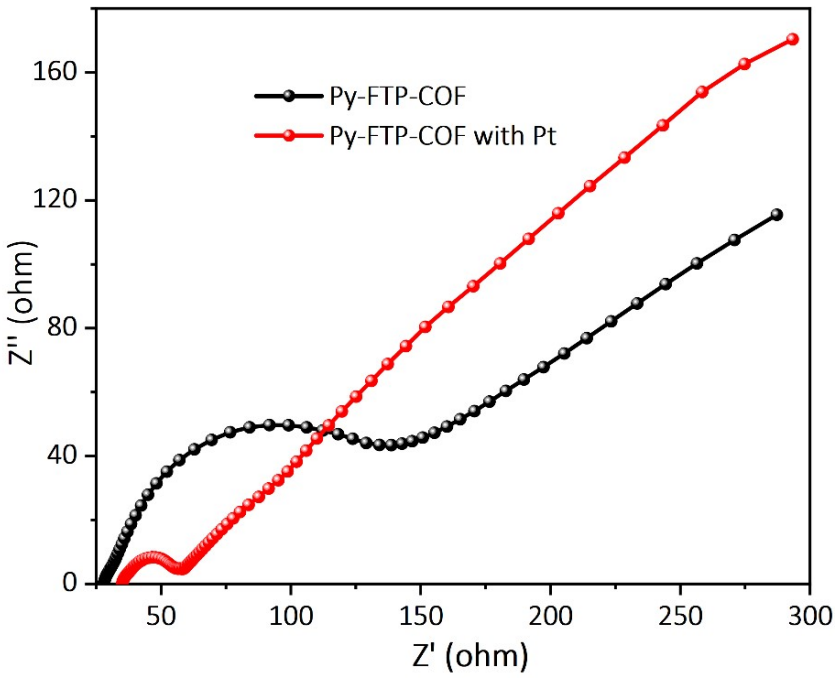

Figure S19. Electrochemical impedance spectroscopy (EIS) Nyquist plots of the **Py-FTP-COF** with and without the Pt co-catalyst.

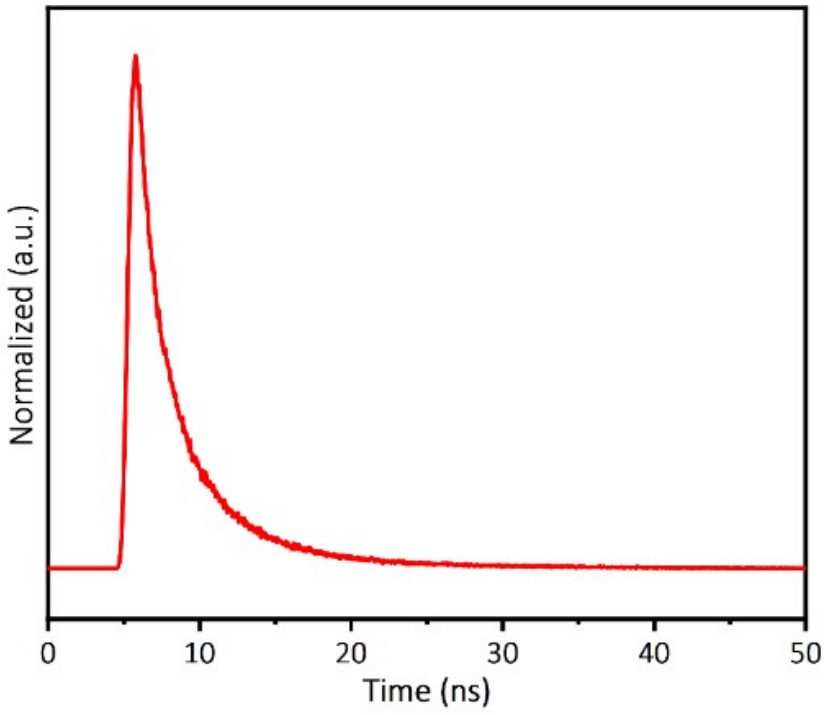

Figure S20. Time-resolved photoluminescence (TRPL) spectrum of the **Py-FTP-COF**. The sample was excited with a 405 nm laser and emission was measured at 630 nm.

Table S3. Optimization of the reaction conditions for the hydrogenation of nitrobenzene catalyzed by **Py-FTP-COF**.

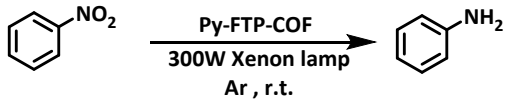

Entry	Py-FTP-COF (mol %)	Solvent (10 mL)	H_2PtCl_6 (μL)	Time (h)	Yield (%)
1	15	H_2A[a] : CH_3OH (3:1)	4	4	20
2	15	H_2A : CH_3OH (1:1)	4	4	85
3	15	H_2A : CH_3OH (1:3)	4	4	Trace
4	15	H_2A : Acetone (1:1)	4	4	60
5	15	H_2A : Ethanol (1:1)	4	4	52
6	15	H_2A : CH_3CN (1:1)	4	4	Trace
7	15	H_2A : CH_3OH (1:1)	4	2	35
8	15	H_2A : CH_3OH (1:1)	8	4	22
9	15	H_2A : CH_3OH (1:1)	4	6	82
10	15	H_2A : CH_3OH (1:1)	2	4	47
11	--	H_2A : CH_3OH (1:1)	4	4	Trace
12	15	H_2A : CH_3OH (1:1)	--	4	Trace
13	30	H_2A : CH_3OH (1:1)	8	4	81
14	6	H_2A : CH_3OH (1:1)	2	4	54
15	15 (blue LED)	H_2A : CH_3OH (1:1)	4	4	25
16	15 (Green LED)	H_2A : CH_3OH (1:1)	4	4	38
17	15 (0.05mmol NB)	H_2A : CH_3OH (1:1)	4	4	85
18	15 (0.2mmol NB)	H_2A : CH_3OH (1:1)	4	4	65

a: H_2A, 0.1 M ascorbic acid water solution; NB: Nitrobenzene

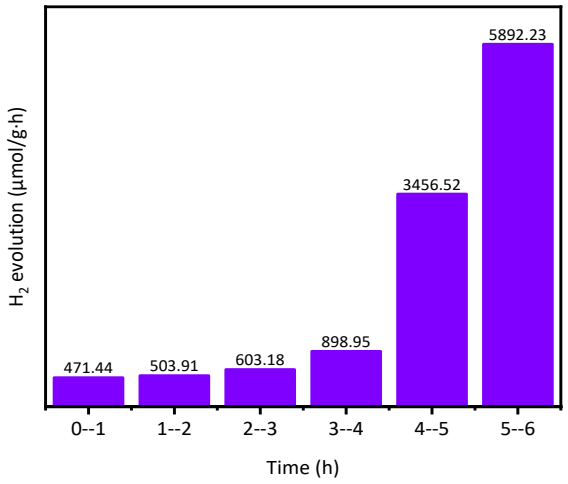

Figure S21. Photocatalytic hydrogen evolution performance of the **Py-FTP-COF** in the presence of nitrobenzene under 300 W Xe lamp irradiation.

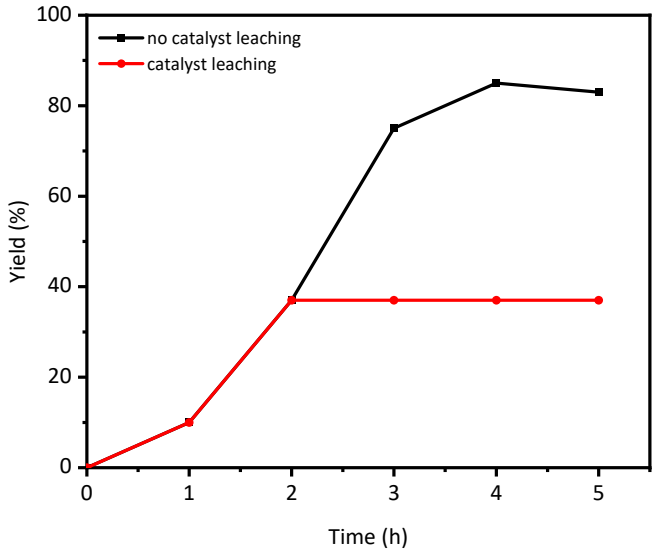

Figure S22. Reaction time examination (black line) and leaching test (red line). The solid catalyst was filtrated from the reaction solution after 2 h, and the filtrate was transferred to a new vial and the reaction was carried out under the same conditions for another 3 h.

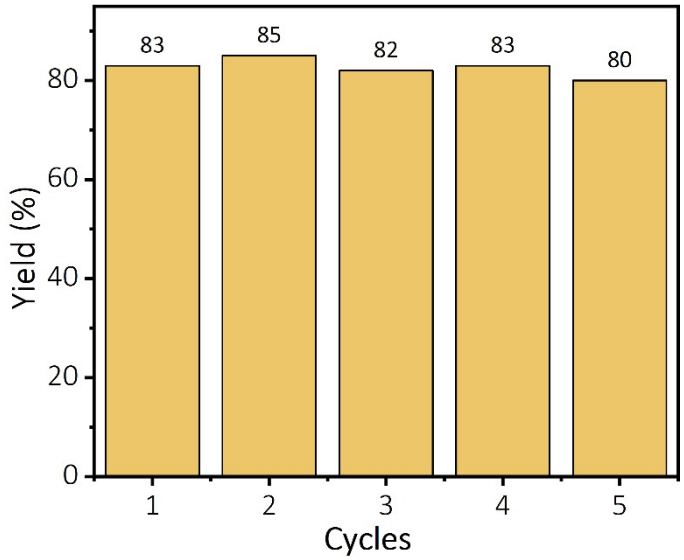

Figure S23. Assessment of the reusability of **Py-FTP-COF** for the hydronation reactions and keep good catalytic effect in 5 cycles.

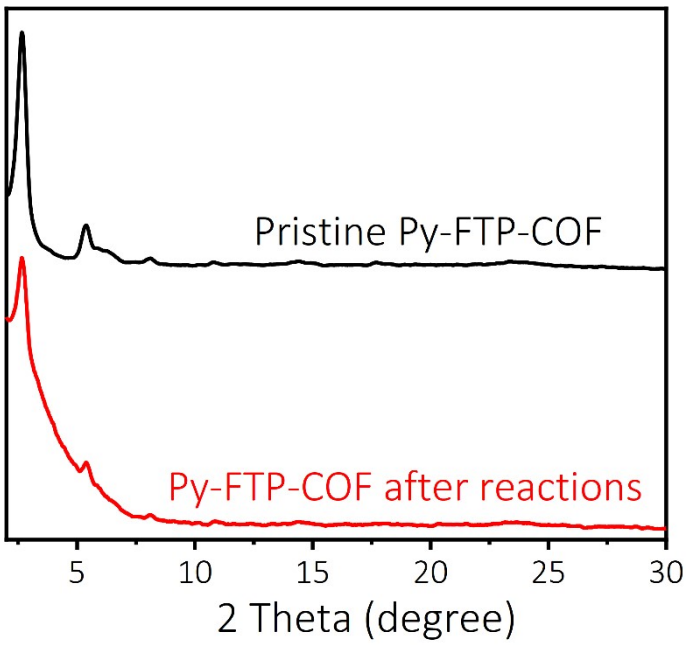

Figure S24. Comparison of the PXRD patterns of **Py-FTP-COF** before and after hydrogenation reactions.

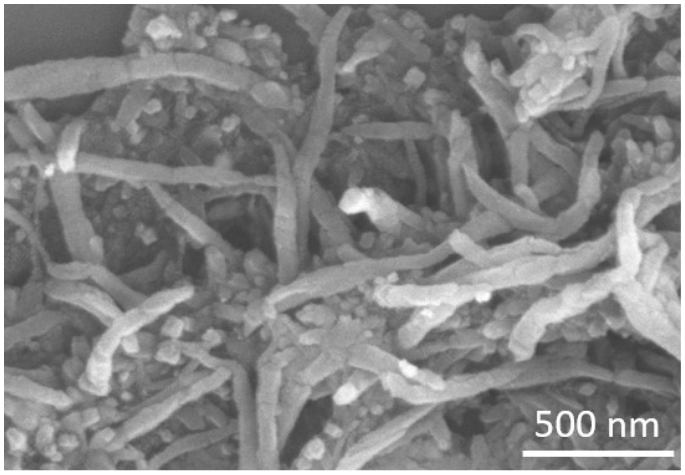

Figure S25. SEM image of the **Py-FTP-COF** after 5 catalytic cycles.

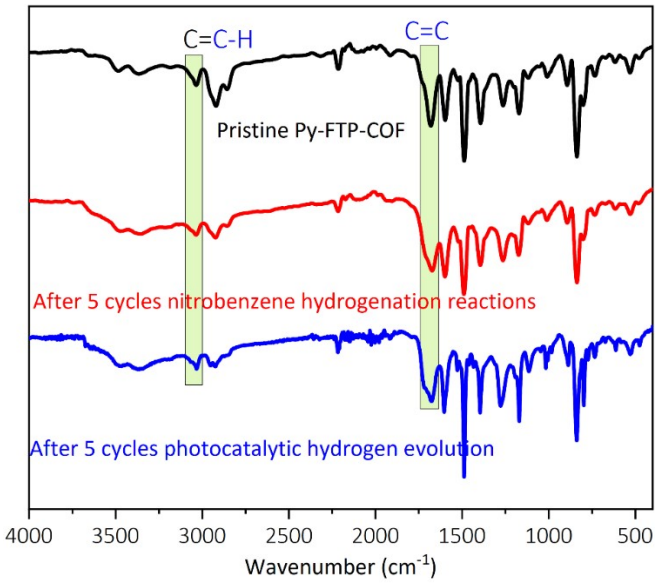

Figure S26. Comparison of the FT-IR spectra of the pristine **Py-FTP-COF** (black), after 5 cycles photocatalytic hydrogen evolution (blue), and after 5 cycles nitrobenzene hydrogenation reactions (red). The characteristic peaks at 3030 cm^{-1} (C=C-H) and 1660 cm^{-1} (C=C) together with the cyano groups (2215 cm^{-1}) were well reserved, confirming that the cyano-vinylene-linkages of the frameworks was not reduced in our case.

Characterization date for all compounds.

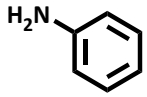

2a

Aniline（2a）：

The product is isolated by column chromatography on silica gel as transparent liquid (isolated yield: 85%), R_f (petroleum ether/ethyl acetate 5:1) = 0.4, ^{1}H NMR (400 MHz, DMSO-d_6) δ 6.99 (t, J = 7.8 Hz, 2H), 6.63 – 6.41 (m, 3H), 4.98 (s, 2H). ^{13}C NMR (101 MHz, Chloroform-d) δ 146.40, 129.33, 118.61. HRMS (ESI) calculated for C_6H_7NNa [M + Na]: 116.0476, Found: 116.0472.

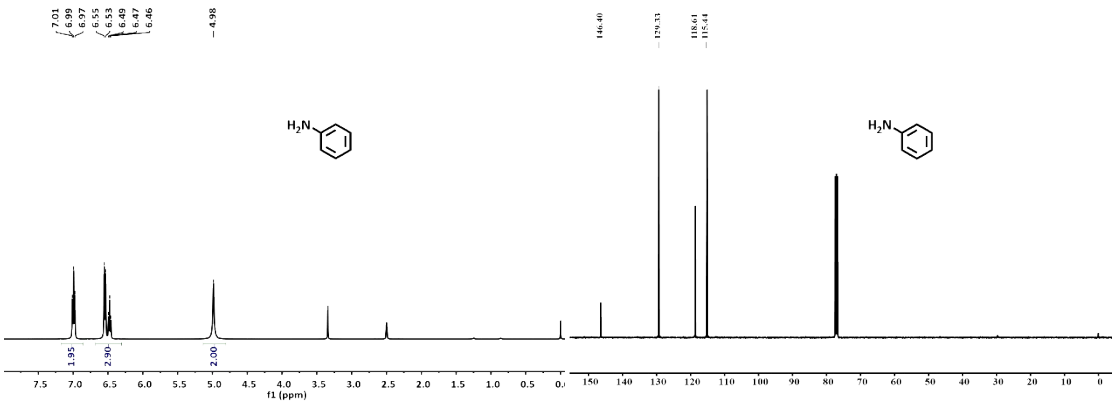

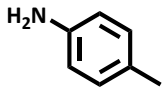

2b

p-Toluidine（2b）：

The product is isolated by column chromatography on silica gel as colorless solid (isolated yield: 91%), R_f (petroleum ether/ethyl acetate 5:1) = 0.4, ^{1}H NMR (400 MHz, DMSO-d_6) δ 6.81 (d, J = 8.0 Hz, 2H), 6.46 (dd, 2H), 4.77 (s, 3H), 2.11 (s, 2H). ^{13}C NMR (101 MHz, Chloroform-d) δ 143.77, 129.77, 127.86, 115.30, 20.45. HRMS (ESI) calculated for $C_7H_{10}N$ [M + H]: 108.0813, Found: 108.0802.

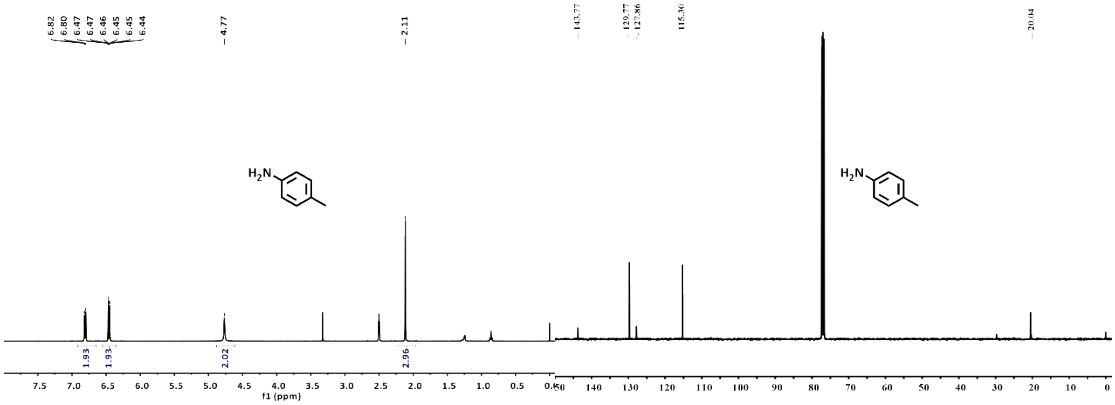

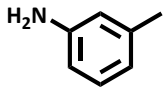

2c

m-Toluidine（2c）：

The product is isolated by column chromatography on silica gel as colorless liquid

(isolated yield: 89%), R_f (petroleum ether/ethyl acetate 5:1) = 0.4, ^{1}H NMR (400 MHz, DMSO-d_6) δ 6.87 (t, *J* = 7.6 Hz, 1H), 6.54 – 6.21 (m, 3H), 4.90 (s, 2H), 2.14 (s, 3H). ^{13}C NMR (101 MHz, Chloroform-*d*) δ 146.32, 139.15, 129.19, 119.50, 115.96, 112.29, 21.46. HRMS (ESI) calculated for $C_7H_{10}N$ [M + H]: 108.0813, Found: 108.0804.

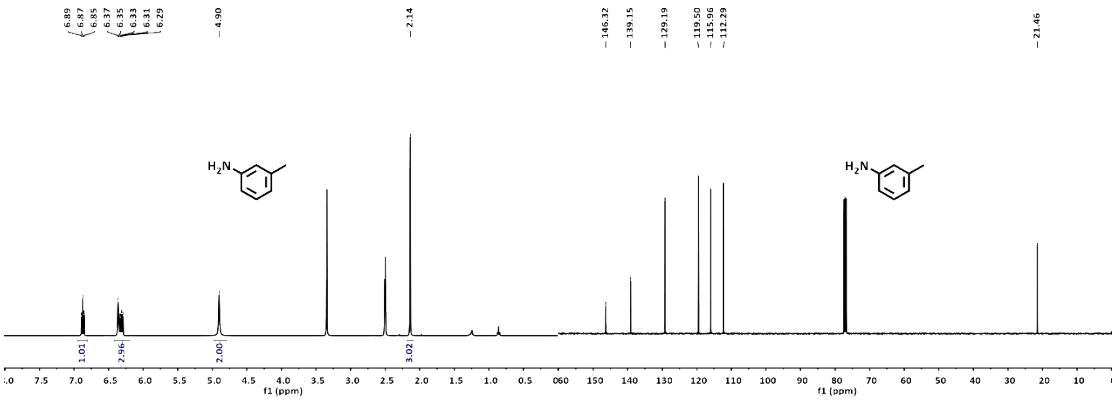

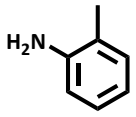

2d

o-Toluidine（2d）：

The product is isolated by column chromatography on silica gel as pale yellow liquid (isolated yield: 90%), R_f (petroleum ether/ethyl acetate 5:1) = 0.4, ^{1}H NMR (400 MHz, DMSO-d_6) δ 6.96 – 6.82 (m, 2H), 6.58 (d, *J* = 7.8 Hz, 1H), 6.44 (t, *J* = 7.3 Hz, 1H), 4.76 (s, 2H), 2.03 (s, 3H). ^{13}C NMR (101 MHz, Chloroform-*d*) δ 144.56, 130.47, 126.99, 122.36, 118.67, 114.97, 17.39. HRMS (ESI) calculated for $C_7H_{10}N$ [M + H]: 108.0813, Found: 108.0798.

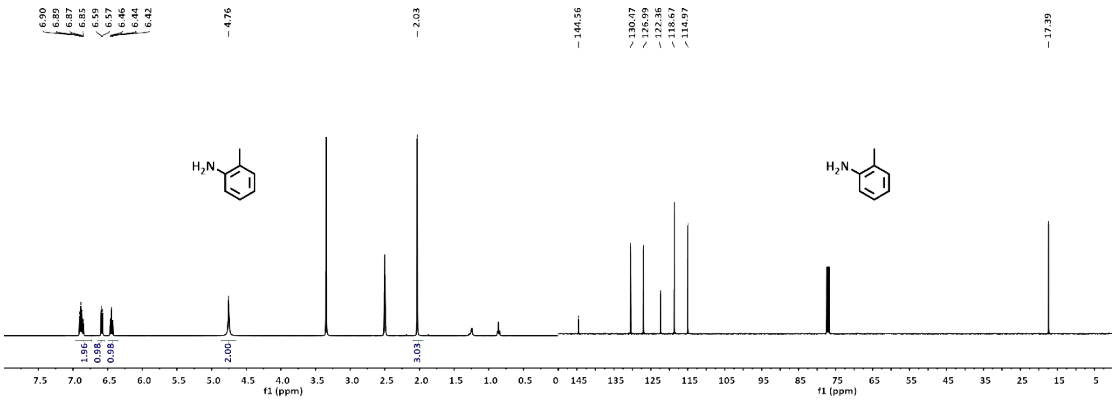

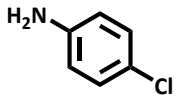

2e

4-Chloroaniline（2e）：

The product is isolated by column chromatography on silica gel as white solid (isolated yield: 79%), R_f (petroleum ether/ethyl acetate 5:1) = 0.4, ^{1}H NMR (400 MHz, DMSO-d_6) δ 7.14 – 6.92 (m, 2H), 6.65 – 6.39 (m, 2H), 5.22 (s, 2H). ^{13}C NMR (101 MHz, Chloroform-*d*) δ 144.96, 129.13, 123.18, 116.24. HRMS (ESI) calculated for C_6H_5ClN [M - H]: 126.0111, Found: 126.0090.

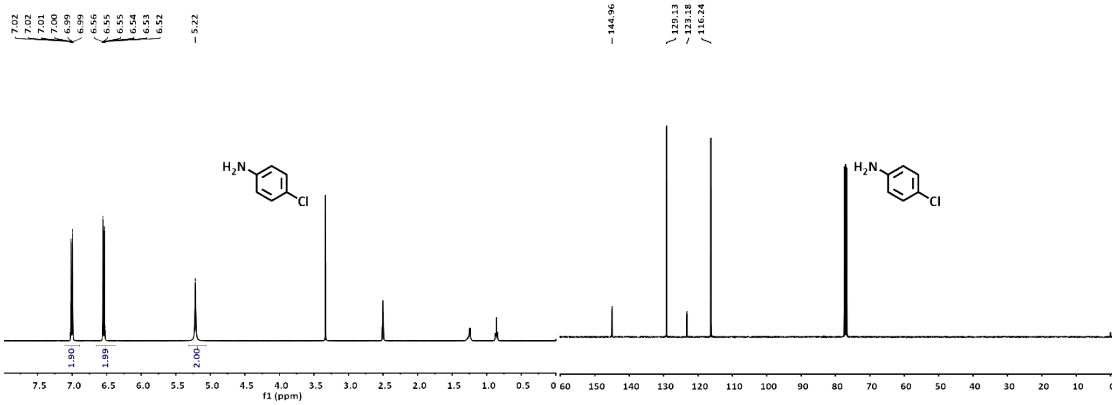

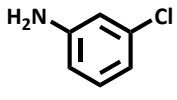

2f

3-Chloroaniline（2f）：

The product is isolated by column chromatography on silica gel as pale yellow liquid

(isolated yield: 74%), R_f (petroleum ether/ethyl acetate 5:1) = 0.4, ^{1}H NMR (400 MHz, DMSO-d_6) δ 6.99 (t, J = 8.0 Hz, 1H), 6.61 – 6.55 (m, 1H), 6.48 (dt, J = 7.7, 2.8 Hz, 2H), 5.38 (s, 2H). ^{13}C NMR (101 MHz, Chloroform-d) δ 147.63, 134.86, 130.33, 118.48, 114.94, 113.20. HRMS (ESI) calculated for C_6H_5ClN [M - H]: 126.0111, Found: 126.0109.

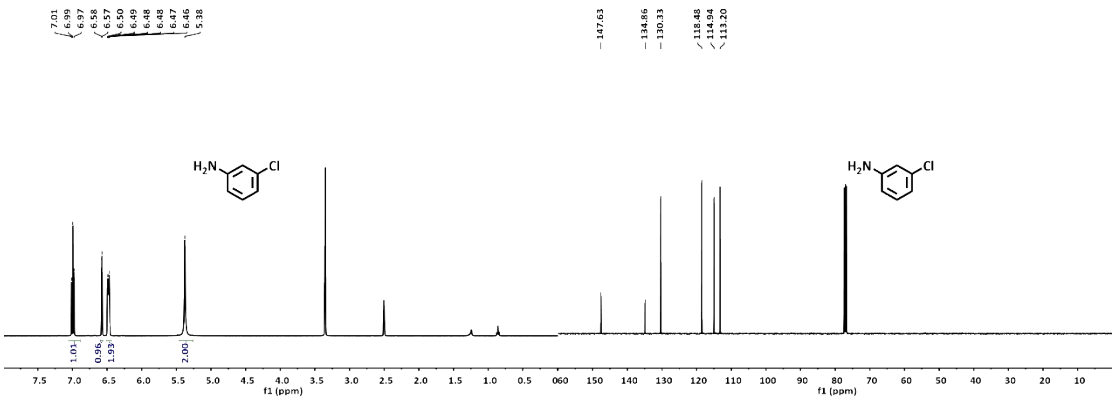

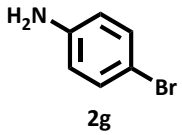

2g

4-Bromoaniline（2g）：

The product is isolated by column chromatography on silica gel as grey solid (isolated yield: 72%), R_f (petroleum ether/ethyl acetate 5:1) = 0.4, ^{1}H NMR (400 MHz, DMSO-d_6) δ 7.24 – 7.05 (m, 2H), 6.62 – 6.37 (m, 2H), 5.25 (s, 2H). ^{13}C NMR (101 MHz, Chloroform-d) δ 145.44, 132.04, 116.73, 110.23. HRMS (ESI) calculated for C_6H_5BrN [M - H]: 169.9606, Found: 169.9594.

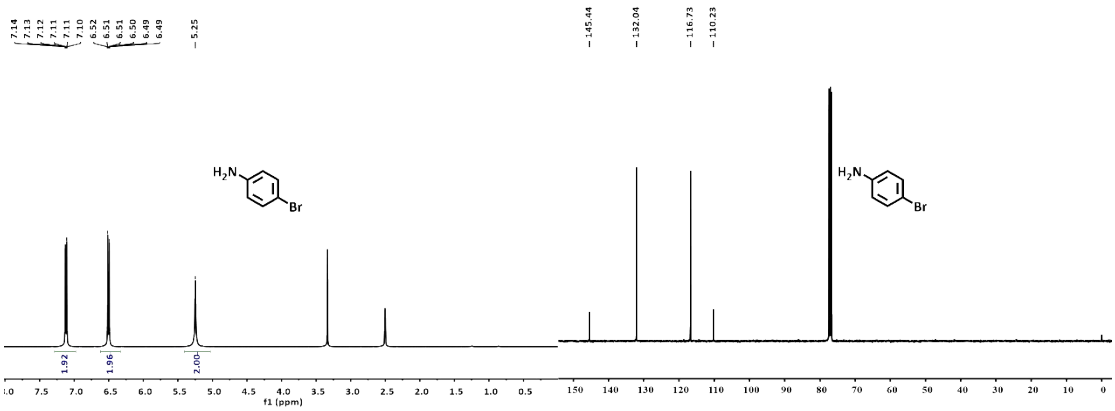

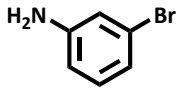

2h

3-Bromoaniline（2h）：

The product is isolated by column chromatography on silica gel as yellow liquid (isolated yield: 70%), R_f (petroleum ether/ethyl acetate 5:1) = 0.4, ^{1}H NMR (400 MHz, DMSO-d_6) δ 6.94 (t, *J* = 8.0 Hz, 1H), 6.73 (s, 1H), 6.61 (dd, *J* = 7.8, 1.7 Hz, 1H), 6.52 (dd, *J* = 8.1, 2.0 Hz, 1H), 5.37 (s, 2H). ^{13}C NMR (101 MHz, Chloroform-*d*) δ 146.74, 129.56, 121.99, 120.31, 116.76, 112.58. HRMS (ESI) calculated for C_6H_5BrN [M - H]: 169.9606, Found: 169.9587.

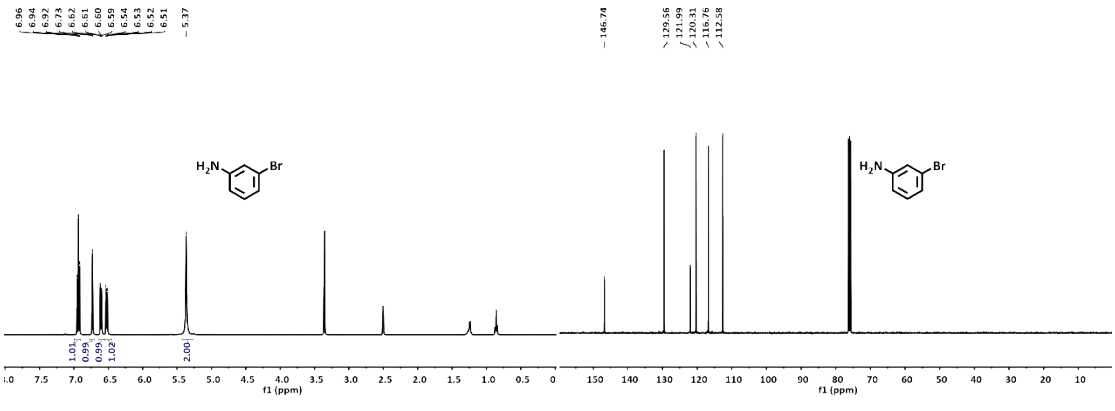

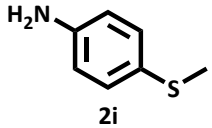

2i

4-(Methylmercapto)aniline（2i）：

The product is isolated by column chromatography on silica gel as black liquid (isolated yield: 92%), R_f (petroleum ether/ethyl acetate 3:1) = 0.4, ^{1}H NMR (400 MHz, DMSO-d_6) δ 7.16 – 6.93 (m, 2H), 6.64 – 6.41 (m, 2H), 5.15 (s, 2H), 2.32 (s, 3H). ^{13}C NMR (101 MHz, Chloroform-*d*) δ 145.08, 131.11, 125.89, 115.75, 18.82. HRMS (ESI) calculated for $C_7H_{10}NS$ [M + H]: 140.0534, Found: 140.0513.

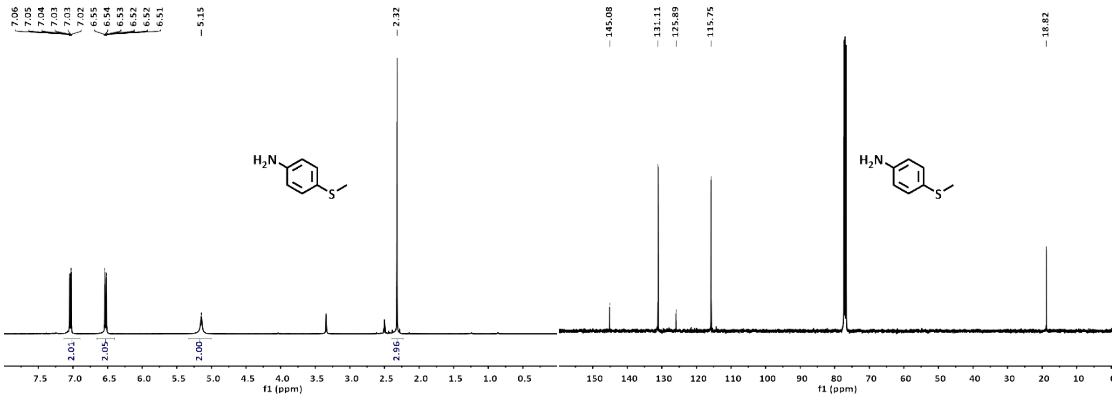

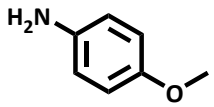

2j

p-Anisidine（2j）：

The product is isolated by column chromatography on silica gel as dark grey solid (isolated yield: 87%), R_f (petroleum ether/ethyl acetate 3:1) = 0.5, ^{1}H NMR (400 MHz, DMSO-d_6) δ 6.69 – 6.61 (m, 2H), 6.55 – 6.49 (m, 2H), 4.60 (s, 2H), 3.62 (s, 3H). ^{13}C NMR (101 MHz, Chloroform-*d*) δ 152.86, 139.92, 116.43, 114.85, 55.76. HRMS (ESI) calculated for $C_7H_{10}NO$ [M + H]: 124.0762, Found: 124.0742.

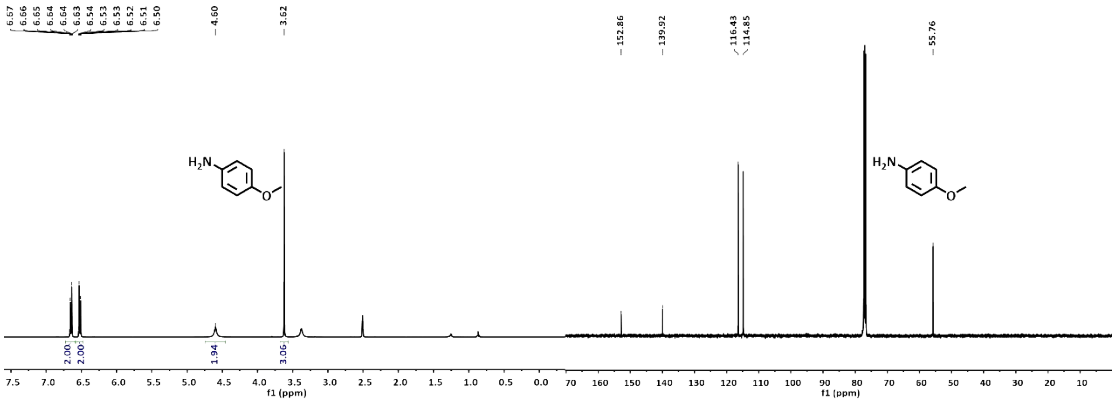

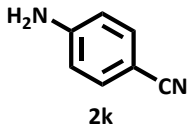

2k

4-Aminobenzonitrile（2k）：

The product is isolated by column chromatography on silica gel as pale yellow solid (isolated yield: 88%), R_f (petroleum ether/ethyl acetate 2:1) = 0.4, 1H NMR (400 MHz, DMSO-d6) δ 7.38 (dd, 2H), 6.60 (dd, 2H), 6.14 (s, 2H)., 4.14 (s, 2H). ^{13}C NMR (101 MHz, Chloroform-*d*) δ 150.38, 133.82, 120.10, 114.45, 100.28. HRMS (ESI) calculated for $C_7H_6N_2Na$ [M + Na]: 141.0429, Found: 141.0409.

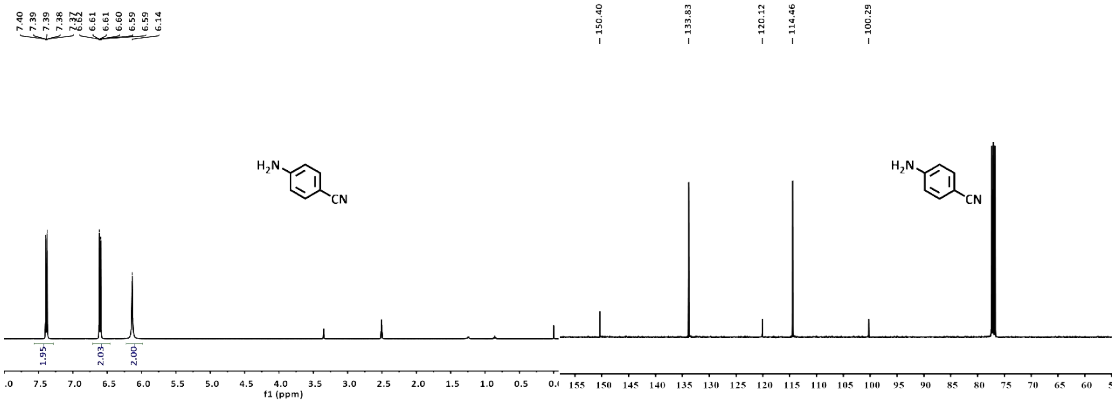

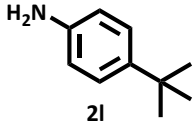

2l

4-tert-Butylaniline（2l）：

The product is isolated by column chromatography on silica gel as pale yellow liquid

(isolated yield: 80%), R_f (petroleum ether/ethyl acetate 5:1) = 0.3, ^{1}H NMR (400 MHz, DMSO-d_6) δ 7.15 – 6.92 (m, 2H), 6.63 – 6.40 (m, 2H), 4.83 (s, 2H), 1.20 (s, 9H). ^{13}C NMR (101 MHz, Chloroform-*d*) δ 143.15, 141.86, 126.08, 115.26, 33.95, 31.52. HRMS (ESI) calculated for $C_{10}H_{16}N$ [M + H]: 150.1283, Found: 150.1263.

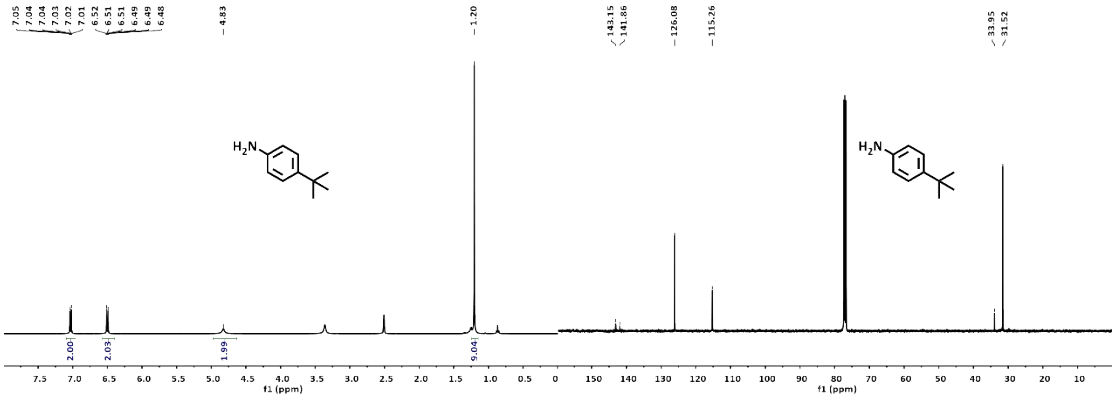

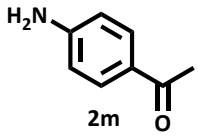

4-Aminoacetophenone（2m）：

The product is isolated by column chromatography on silica gel as yellow solid (isolated yield: 82%), R_f (petroleum ether/ethyl acetate 2:1) = 0.5, ^{1}H NMR (400 MHz, DMSO-d_6) δ 7.66 (d, *J* = 8.4 Hz, 2H), 6.55 (d, *J* = 8.5 Hz, 2H), 6.03 (s, 2H), 2.38 (s, 3H). ^{13}C NMR (101 MHz, Chloroform-*d*) δ 196.50, 151.17, 130.80, 127.85, 113.72, 26.08. HRMS (ESI) calculated for C_8H_9NONa [M + Na]: 158.0582, Found: 158.0561.

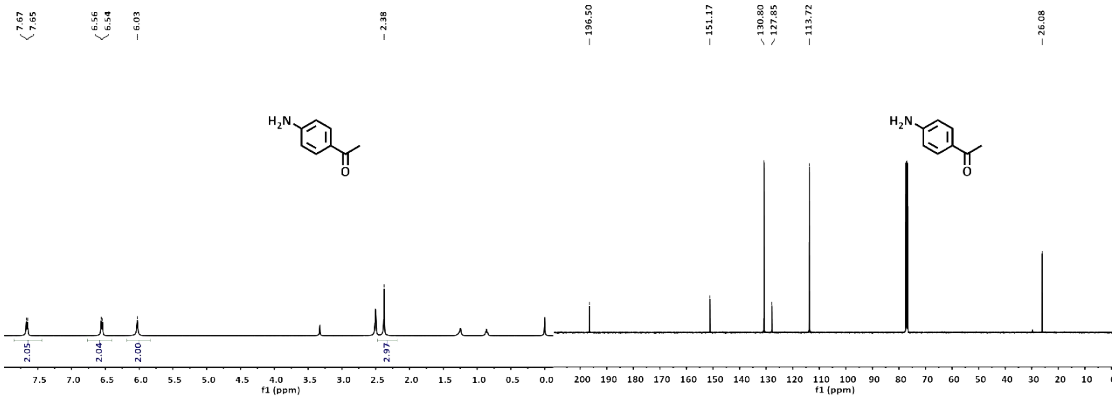

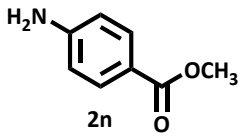

2n

Methyl 4-aminobenzoate（2n）：

The product is isolated by column chromatography on silica gel as white solid (isolated yield: 95%), R_f (petroleum ether/ethyl acetate 2:1) = 0.4, ^{1}H NMR (400 MHz, DMSO-d_6) δ 7.63 (d, J = 8.7 Hz, 2H), 6.56 (d, J = 8.7 Hz, 2H), 5.97 (s, 2H), 3.72 (s, 3H). ^{13}C NMR (101 MHz, $CDCl_3$) δ 167.17, 150.81, 131.60, 119.76, 113.81, 51.61. HRMS (ESI) calculated for $C_8H_8NO_2$ [M - H]: 150.0555, Found: 150.0536.

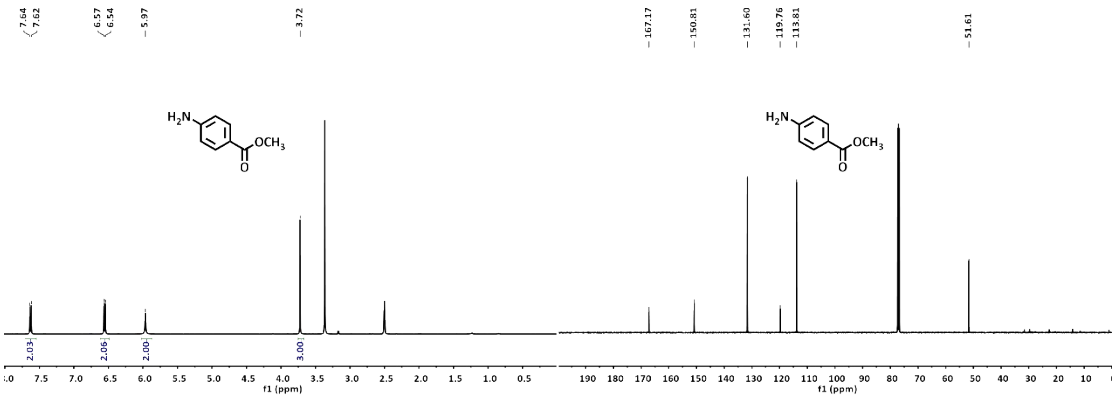

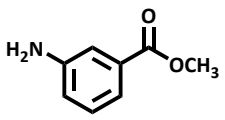

2o

Methyl 3-aminobenzoate（2o）：

The product is isolated by column chromatography on silica gel as grey solid (isolated yield: 88%), R_f (petroleum ether/ethyl acetate 2:1) = 0.4, ^{1}H NMR (400 MHz, DMSO-d_6) δ 7.22 – 7.18 (m, 1H), 7.14 (t, J = 7.6 Hz, 1H), 7.11 – 7.07 (m, 1H), 6.80 (ddd, J = 7.7, 2.4, 1.4 Hz, 1H), 5.40 (s, 2H), 3.80 (s, 3H). ^{13}C NMR (101 MHz, Chloroform-d) δ 167.28, 146.40, 131.14, 129.27, 119.75, 119.43, 115.81, 52.04. HRMS (ESI) calculated for $C_8H_8NO_2$ [M - H]: 150.0555, Found: 150.0533.

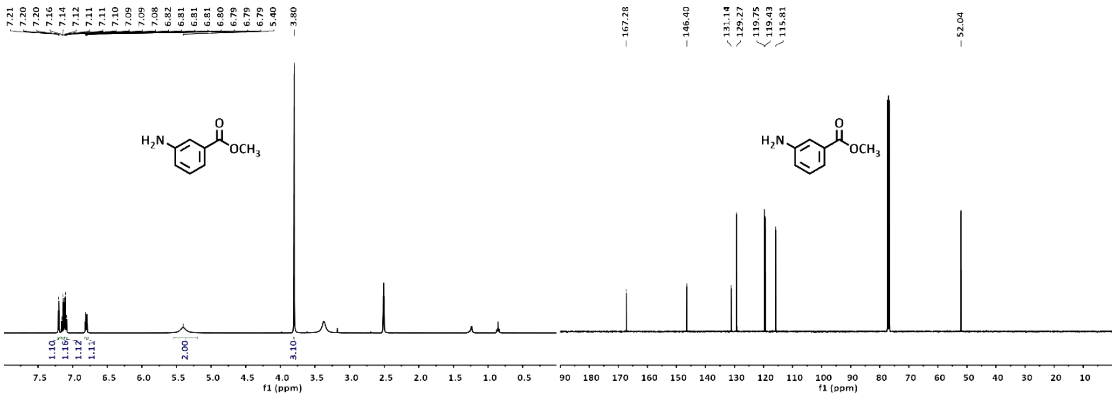

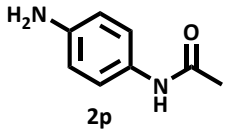

2p

4'-Aminoacetanilide（2p）：

The product is isolated by column chromatography on silica gel as grey solid (isolated yield: 93%), R_f (petroleum ether/ethyl acetate 1:1) = 0.2, ^{1}H NMR (400 MHz, DMSO-d_6) δ 9.48 (s, 1H), 7.18 (d, *J* = 8.6 Hz, 2H), 6.48 (d, *J* = 8.6 Hz, 2H), 4.81 (s, 2H), 1.95 (s, 3H). ^{13}C NMR (101 MHz, DMSO-d_6) δ 167.63, 145.03, 129.03, 121.27, 114.23, 24.15. HRMS (ESI) calculated for $C_8H_9N_2O$ [M - H]: 149.0715, Found: 149.0686.

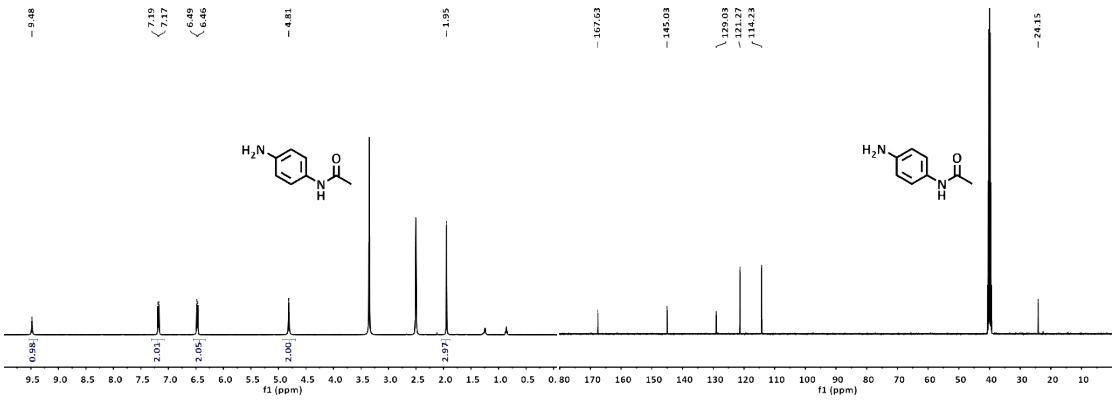

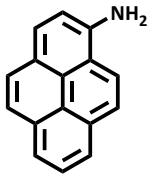

2q

1-Aminopyrene（2q）：

The product is isolated by column chromatography on silica gel as yellow solid (isolated yield: 83%), R_f (petroleum ether/ethyl acetate 5:1) = 0.4,^{1}H NMR (400 MHz, DMSO-d_6) δ 8.26 (d, *J* = 9.2 Hz, 1H), 7.98 (t, *J* = 9.2 Hz, 3H), 7.93 – 7.84 (m, 3H), 7.71 (d, *J* = 8.8 Hz, 1H), 7.37 (d, *J* = 8.3 Hz, 1H), 6.34 (s, 2H). ^{13}C NMR (101 MHz, Chloroform-*d*) δ 140.89, 132.20, 131.65, 127.61, 126.01 (d, *J* = 6.8 Hz), 125.50, 124.30, 124.11, 123.75, 123.55, 120.15, 116.88, 113.96. HRMS (ESI) calculated for $C_{16}H_{11}N$ [M - H]: 216.0813, Found: 216.0786.

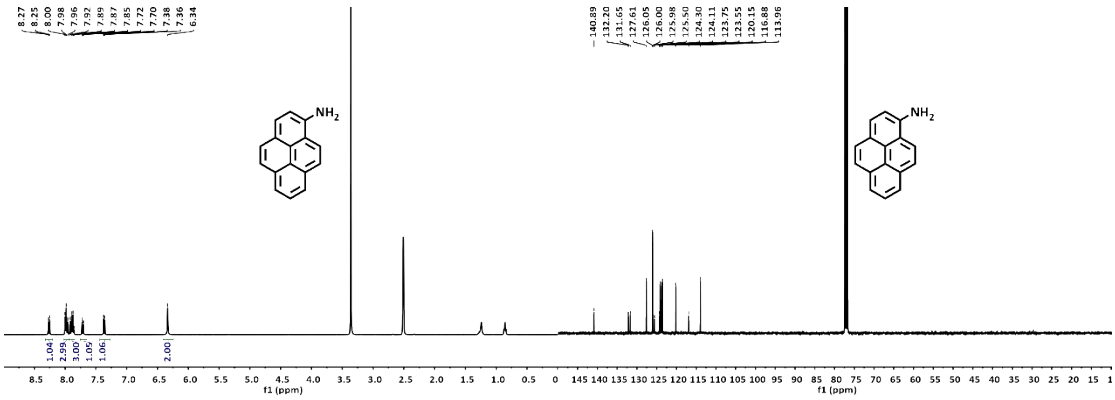

Reference

1. S. Bi, C. Yang, W. Zhang, J. Xu, L. Liu, D. Wu, X. Wang, Y. Han, Q. Liang and F. Zhang, *Nat. Commun.*, 2019, **10**, 2467.
2. C. Liu, Y. Xiao, Q. Yang, Y. Wang, R. Lu, Y. Chen, C. Wang and H. Yan, Appl. Surf. Sci., 2021, **537**.
3. V. S. Vyas, F. Haase, L. Stegbauer, G. Savasci, F. Podjaski, C. Ochsenfeld and B. V. Lotsch, *Nat. Commun.*, 2015, **6**, 8508.
4. J. Thote, H. B. Aiyappa, A. Deshpande, D. Díaz Díaz, S. Kurungot and R. Banerjee, *Chem. Eur. J.*, 2014, **20**, 15961.
5. H. Dong, X.-B. Meng, X. Zhang, H.-L. Tang, J.-W. Liu, J.-H. Wang, J.-Z. Wei, F.-M. Zhang, L.-L. Bai and X.-J. Sun, *Chem. Eng. J.*, 2020, **379**, 122342.
6. W. Dong, Z. Qin, K. Wang, Y. Xiao, X. Liu, S. Ren, L. Li, *Angew. Chem. Int. Ed*, 2022, e202216073.
7. S. Wei, F. Zhang, W. Zhang, P. Qiang, K. Yu, X. Fu, D. Wu, S. Bi, F. Zhang, *J. Am. Chem. Soc.* 2019, **141**, 14272.
8. J. Ming, A. Liu, J. Zhao, P. Zhang, H. Huang, H. Lin, Z. Xu, X. Zhang, X. Wang, J. Hofkens, M. B. J. Roeffaers and J. Long, *Angew. Chem. Int. Ed.*, 2019, **58**, 18290.
9. F. Haase, T. Banerjee, G. Savasci, C. Ochsenfeld and B. V. Lotsch, *Faraday Discuss.*, 2017,

201, 247.
10. T. Banerjee, F. Haase, G. Savasci, K. Gottschling, C. Ochsenfeld and B. V. Lotsch, *J. Am. Chem. Soc.*, 2017, **139**, 16228.
11. Z.-A. Lan, Y. Fang, X. Chen and X. Wang, *Chem. Commun.*, 2019, **55**, 7756.
12. E. Jin, Z. Lan, Q. Jiang, K. Geng, G. Li, X. Wang and D. Jiang, *Chem*, 2019, **5**, 1632.
13. L. Y. Li, Z. M. Zhou, L. Y. Li, Z. Y. Zhuang, J. H. Bi, J. H. Chen, Y. Yu and J. G. Yu, *ACS Sustain. Chem. Eng.*, 2019, **7**, 18574.
14. S. Bi, Z.-A. Lan, S. Paasch, W. Zhang, Y. He, C. Zhang, F. Liu, D. Wu, X. Zhuang, E. Brunner, X. Wang and F. Zhang, *Adv. Funct. Mater.*, 2017, **27**, 1703146.
15. F. Li, D. Wang, Q.-J. Xing, G. Zhou, S.-S. Liu, Y. Li, L.-L. Zheng, P. Ye and J.-P. Zou, *Appl. Catal. B: Environ.*, 2019, **243**, 621.
16. J.-L. Sheng, H. Dong, X.-B. Meng, H.-L. Tang, Y.-H. Yao, D.-Q. Liu, L.-L. Bai, F.-M. Zhang, J.-Z. Wei and X.-J. Sun, *ChemCatChem*, 2019, **11**, 2313.
17. P. Pachfule, A. Acharjya, J. Roeser, T. Langenhahn, M. Schwarze, R. Schomäcker, A. Thomas and J. Schmidt, *J. Am. Chem. Soc.*, 2018, **140**, 1423.
18. C. B. Meier, R. Clowes, E. Berardo, K. E. Jelfs, M. A. Zwijnenburg, R. S. Sprick and A. I. Cooper, *Chem. Mater.*, 2019, **31**, 8830.
19. A. F. M. El-Mahdy, A. M. Elewa, S.-W. Huang, H.-H. Chou and S.-W. Kuo, *Adv. Opt. Mater.*, 2020, **8**.
20. R. Lu, C. Liu, Y. Chen, L. Tan, G. Yuan, P. Wang, C. Wang, H. Yan, *Journal of Photochemistry*., 2021, **421**, 113546.
21. X. Wu, M. Zhang, Y. Xia, C. Ru, P. Chen, H. Zhao, L. Zhou, C. Gong, J. Wu, X. Pan, ***J. Mater. Chem. A.,*** 2022, **10**, 17691.
22. S. Ghosh, A. Nakada, M. A. Springer, T. Kawaguchi, K. Suzuki, H. Kaji, I. Baburin, A. Kuc, T. Heine, H. Suzuki, R. Abe and S. Seki, *J. Am. Chem. Soc.*, 2020, **142**, 9752.
23. B. P. Biswal, H. A. Vignolo-González, T. Banerjee, L. Grunenberg, G. Savasci, K. Gottschling, J. Nuss, C. Ochsenfeld and B. V. Lotsch, *J. Am. Chem. Soc.*, 2019, **141**, 11082.
24. G.-B. Wang, S. Li, C.-X. Yan, Q.-Q. Lin, F.-C. Zhu, Y. Geng, Y.-B. Dong, *Chem. Commun*., 2020, **56**, 12612.
25. F.-M. Zhang, J.-L. Sheng, Z.-D. Yang, X.-J. Sun, H.-L. Tang, M. Lu, H. Dong, F.-C. Shen, J. Liu and Y.-Q. Lan, *Angew. Chem. Int. Ed.*, 2018, **57**, 12106.
26. G.-B. Wang, F.-C. Zhu, Q.-Q. Lin, J.-L. Kan, K.-H. Xie, S. Li, Y. Geng, Y.-B. Dong, *Chem. Commun*., 2021, **57**, 4464.
27. X. Wang, L. Chen, S. Y. Chong, M. A. Little, Y. Wu, W.-H. Zhu, R. Clowes, Y. Yan, M. A. Zwijnenburg, R. S. Sprick and A. I. Cooper, *Nat. Chem.*, 2018, **10**, 1180.
28. L. Stegbauer, K. Schwinghammer and B. V. Lotsch, *Chem. Sci.*, 2014, **5**, 2789.
29. W. Li, X. Huang, T. Zeng, Y. A. Liu, W. Hu, H. Yang, Y.-B. Zhang and K. Wen, *Angew. Chem. Int. Ed.*, 2020, **60**, 1869.
30. J. Xu, C. Yang, S. Bi, W. Wang, Y. He, D. Wu, Q. Liang, X. Wang and F. Zhang, *Angew. Chem. Int. Ed.*, 2020, **59**, 23845.
31. W. Chen, L. Wang, D. Mo, F. He, Z. Wen, X. Wu, H. Xu and L. Chen, *Angew. Chem. Int. Ed.*, 2020, **59**, 16902.
32. Y.-P. Zhang, H.-L. Tang, H. Dong, M.-Y. Gao, C.-C. Li, X.-J. Sun, J.-Z. Wei, Y. Qu, Z.-J. Li and F.-M. Zhang, *J. Mater. Chem. A*., 2020, 8, 4334.

33. M. Y. Gao, C. C. Li, H. L. Tang, X. J. Sun, H. Dong and F. M. Zhang, *J. Mater. Chem. A*, 2019, **7**, 20193.
34. M. Luo, Q. Yang, K. Liu, H. Cao and H. Yan, *Chem. Commun.*, 2019, **55**, 5829.
35. C.-C. Li, M.-Y. Gao, X.-J. Sun, H.-L. Tang, H. Dong and F.-M. Zhang, *Appl. Catal. B: Environ.*, 2020, **266**.
36. Y.-H. Yao, J. Li, H. Zhang, H.-L. Tang, L. Fang, G.-D. Niu, X.-J. Sun and F.-M. Zhang, *J. Mater. Chem. A*, 2020, **8**, 8949.
37. Y.-J. Cheng, R. Wang, S. Wang, X.-J. Xi, L.-F. Ma and S.-Q. Zang, *Chem. Commun.*, 2018, **54**, 13563.
38. W. Li, X. Ding, B. Yu, H. Wang, Z. Gao, X. Wang, X. Liu, K. Wang, J. Jiang, *Adv. Funct. Mater*., 2022, **32**, 2207394.
39. H. Yan, Y.-H. Liu, Y. Yang, H.-Y. Zhang, X.-R. Liu, J.-Z. Wei, L.-L. Bai, Y. Wang, F.-M. Zhang, *Chem. Eur. J.*, **431**, 133404.
40. Z. Mi, T. Zhou, W. Weng, J. Unruangsri, K. Hu, W. Yang, C. Wang, K. A. I. Zhang, J. Guo, *Angew. Chem. Int. Ed.,* 2021, **60**, 9642.
41. Y. Zang, R. Wang, P.-P. Shao, X. Feng, S. Wang, S.-Q. Zang and T. C. W. Mak, *J. Mater. Chem. A*, 2020, **8**, 25094.
42. S. Ma, T. Deng, Z. Li, Z. Zhang, J. Jia, Q. Li, G. Wu, H. Xia, S.-W. Yang, X. Liu, *Angew. Chem. Int. Ed*., 2022, **61**, e202208919.